PURIFICATION AND CHARACTERIZATION OF THE *DANAUS PLEXIPPUS* CRYPTOCHROMES

Tracy R. Denaro

A thesis submitted to the faculty of the University of North Carolina at Chapel Hill in partial fulfillment of the requirements for the degree of Master of Science in the Department of Biochemistry and Biophysics.

Chapel Hill

2006

Approved by

Aziz Sancar, M.D., Ph.D.

Gwendolyn Sancar, Ph.D.

Richard Wolfenden, Ph.D.

ABSTRACT

Tracy R. Denaro: Purification and Characterization of the *Danaus Plexippus* Cryptochromes

(Under the direction of Dr. Aziz Sancer)

Cryptochromes are flavoproteins that function as blue-light photoreceptors to regulate growth in plants and to entrain the circadian clock in animals. The photochemical and signaling mechanisms by which cryptochromes function are still undefined. Two cryptochromes identified in *Danaus plexippus* have shown distinct *in vivo* activities where DpCry1 is similar to *Drosophila melanogaster* cryptochrome and DpCry2 is similar to mammalian cryptochromes. I purified and biochemically characterized both *D. plexippus* cryptochromes. DpCry1 is the first animal cryptochrome to contain near-stoichiometric flavin. Photoreduction of FAD_{ox} to $FAD^{\circ-}$ and fluorescence lifetime measurements showing an extremely short lifetime of flavin in DpCry1 both suggest a novel photochemical mechanism for DpCry1. DpCry2 contained only trace amounts of flavin and both proteins contained sub-stoichiometric MTHF. Purification of DpCry1 as the first animal cryptochrome with near-stoichiometric flavin will enable crucial *in vitro* biochemical and biophysical experiments that have never been conducted on an animal cryptochrome.

To my dad, one of the smartest men I know, who has not only been an incredible inspiration to me, but who has given me much needed personal and professional guidance for as long as I can remember…

ACKNOWLEDGEMENTS

All of the work presented in this thesis was made feasible by the direction and mentoring of my advisor, Dr. Aziz Sancar. He provided crucial direction and instruction while maintaining high expectations to challenge me and thus allow me to reach my full potential. I would like to thank the remaining members of my committee, Dr. Gwendolyn Sancar, who was very helpful during the writing of my thesis, and Dr. Richard Wolfenden. I would like to thank our collaborators, Dr. Steven Reppert who donated the *Danaus plexippus* clones and Dr. Dongping Zhong who conducted the photophysical analysis of DpCry1 for their important contributions to my thesis work. I would also like to thank my coworker, Dr. Sang-Hun Song, who conducted some of the spectroscopic experiments. Additionally, the remaining members of the Sancar lab, specifically Dr. Christopher Selby, Dr. Laura Lindsey-Boltz, Dr. Joyce Reardon, Michele Gauger, and Lydia Morrison, were very helpful as they shared their expertise and knowledge throughout the duration of my experiments.

I would like to thank the Air Force for their funding; giving me the opportunity to expand my knowledge and become a better US Air Force officer.

Finally I would like to thank my fiancé and my parents for their continuous support and encouragement.

TABLE OF CONTENTS

LIST OF FIGURES

FIGURE

CHAPTER 1

INTRODUCTION

Summary

Cryptochromes are found in species ranging from bacteria to mammals and are essential components to the central circadian clock, the disruption of which can lead to serious health disorders including delayed sleep phase syndrome, seasonal affective disorder, and cancer. They are members of the photolyase/cryptochrome family of structurally similar flavoproteins which are best classified as blue-light photoreceptors that repair UV-induced DNA damage (photolyase), regulate growth (plant cryptochrome), or align the circadian clock with daily light/dark cycles (mammalian cryptochrome). Proteins within this family generally contain two cofactors, the catalytic flavin adenine dinucleotide (FAD) and the photoantenna, most commonly methenyltetrahydrofolate (MTHF). The photocycle of photolyase is well characterized; however the photocycle of cryptochromes has yet to be determined. The moderate sequence homology and high structural homology between these proteins suggests a model for the cryptochrome photocycle, however definitive data to support or refute this model is currently lacking.

Cryptochromes have demonstrated both light-dependent photoreceptor activity (bacteria, insects, and plants) similar to photolyase and light-independent transcriptional repressor activity (mammalian). Recently, two cryptochromes from the monarch butterfly (*Danaus plexippus*) have been identified and cloned. DpCry1 is degraded in response to

light similarly to *Drosophila* cryptochrome (dCry), whereas DpCry2 has shown transcriptional repression of core clock proteins similar to mouse cryptochrome 1 (mCry1). Although *Drosophila* cryptochrome has been the classic animal cryptochrome model, recent phylogenetic data has suggested that the basal insect lineage of cryptochromes is more accurately represented by the *D. plexippus* cryptochromes rather than the *Drosophila* cryptochrome; making further study of DpCry1 and DpCry2 important. The objective of this research was to characterize DpCry1 and DpCry2 using biochemical and biophysical methods.

I hypothesized that DpCry1 has biochemical properties to support light-dependent photoreceptor activity and that DpCry2 has biochemical properties similar to those observed in other mammalian cryptochromes. To test this hypothesis, I cloned and expressed recombinant DpCry1 and DpCry2 from a bacterial expression system and purified them using affinity chromatography under low-stringency conditions to retain chromophores. I assessed the relative chromophore content and the flavin lifetime using spectroscopic and photophysical methods, respectively. I also assessed the relative autophosphorylating kinase activity of each *D. plexippus* cryptochrome.

An important goal of this research was to retain as much flavin as possible in each protein in hopes that we might obtain the first animal cryptochrome with stoichiometric flavin. All animal cryptochromes that have been characterized so far have only trace amounts of flavin. Recombinant cryptochromes with sub-stoichiometric flavin preclude further biophysical studies, making biochemical characterization of flavin-lacking animal cryptochromes very difficult. The lack of flavin in all animal cryptochromes characterized so far has therefore hindered the progress of elucidating the cryptochrome photocycle and

photochemical mechanisms. Identifying the cryptochrome photocycle will greatly contribute to an understanding of how cryptochrome may be related to circadian health disorders and will lead to a better global understanding of the health-related risks inherent to circadian rhythm disruption.

Background

Photolyase/cryptochrome family of blue-light photoreceptors

Cryptochromes are indispensable elements of circadian rhythms: daily physiological and behavioral oscillations with a periodicity of about 24 hours (1). Disruption of normal circadian cycles can lead to health disorders such as delayed sleep phase syndrome and seasonal affective disorder (2). Additional health-related impacts include jet lag and numerous connections to cancer (2). The total number and severity of health-related problems caused by circadian rhythm disruptions is unknown since many molecular details of the process are still undefined. Specifically, identification of the photoreactive pigment and the mechanism by which it aligns our intrinsic circadian rhythm to the surroundings is crucial for a complete understanding of the health-impacts of circadian disruption.

Cryptochromes belong to the photolyase/cryptochrome family of structurally analogous blue-light photoreceptors. Photolyase utilizes blue-light to repair DNA damage such as cyclobutane pyrimidine dimer (Pyr<>Pyr) through a well-characterized photocycle (3-5). Cryptochrome, though structurally similar to photolyase, lacks DNA repair activity and instead employs blue-light to regulate growth and adaptations in plants and to entrain the circadian clock to daily light-dark cycles in animals, using photoreactive mechanisms that

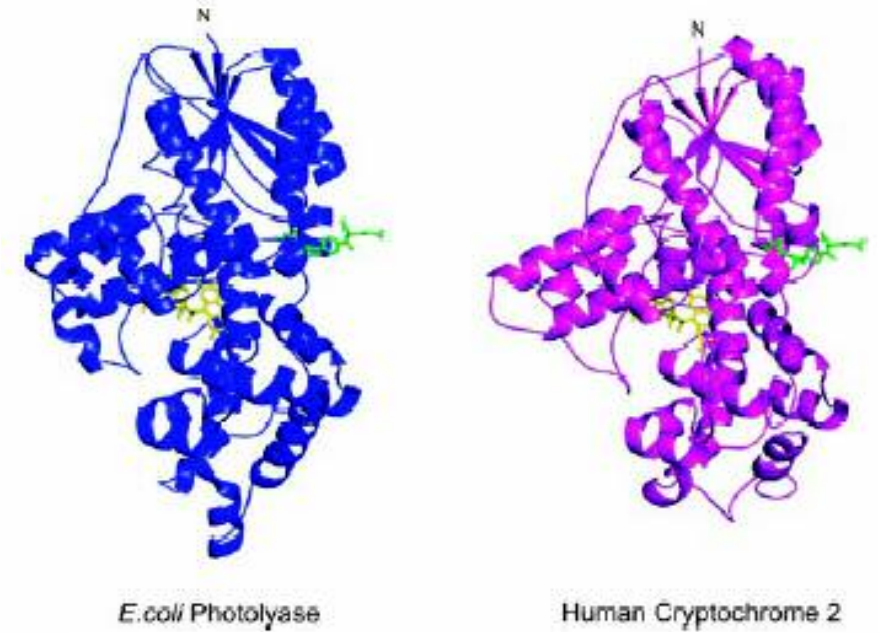

Figure 1. Crystal structure of *E. coli* photolyase and the photolyase-homology region of human cryptochrome 2. The crystal structure of *E. coli* photolyase (left) is shown with non-covalently bound cofactors FAD (yellow) and MTHF (green). A computer-generated model of the photolyase homology domain of human cryptochrome 1 (right) is shown with possible cofactors placed in accordance with the photolyase structure (4).

have yet to be identified. The high structural homology between these proteins suggests the photolyase photocycle as a potential model for the photocycle of cryptochrome (6).

Although cryptochromes contain only 25-40% sequence homology to photolyase, they are very similar structurally (Fig.1) (6). All identified cryptochromes possess a 471 amino acid photolyase-homology region that contains an N-terminal α/β domain and a C-terminal α-helical domain connected by a long interdomain loop (5,7,8). Certain cryptochromes (primarily in eukaryotes) have an additional C-terminal extension that varies in length from 20 to 350 amino acids (6). Two cofactors or chromophores are non-covalently bound to photolyase and to the photolyase homology region of cryptochrome; most commonly 5,10-methenyltetrahydrofolate (MTHF) and flavin adenine dinucleotide (FAD) (1). MTHF, the photoantenna, binds within a cleft between the N- and C-terminal domains of the photolyase-homology region which places the cofactor near the surface of the protein (5). Within the α-helical domain, 16.8 Å away from MTHF, the catalytic FAD is bound in a U-shaped conformation (5).

Photoantenna – MTHF

MTHF was first identified in *E. coli* photolyase by its spectroscopic properties after protein denaturation and HPLC purification (9). The chemical structure and absorption spectra of both free and enzyme-bound MTHF chromophore are illustrated in Figure 2a. The methenyl bridge between the pterin ring and the paraminobenzoic acid creates an absorption peak at 360 nm in free MTHF (Fig 2b) (9). However, polar enzyme interactions around the positively charged methenyl bridge and the hydrophobic enzyme interactions with the pterin ring create a red shift in the absorption spectrum; the extent of which varies among photolyases from different species (Fig. 2c) (10-12). The length of the polyglutamate tail

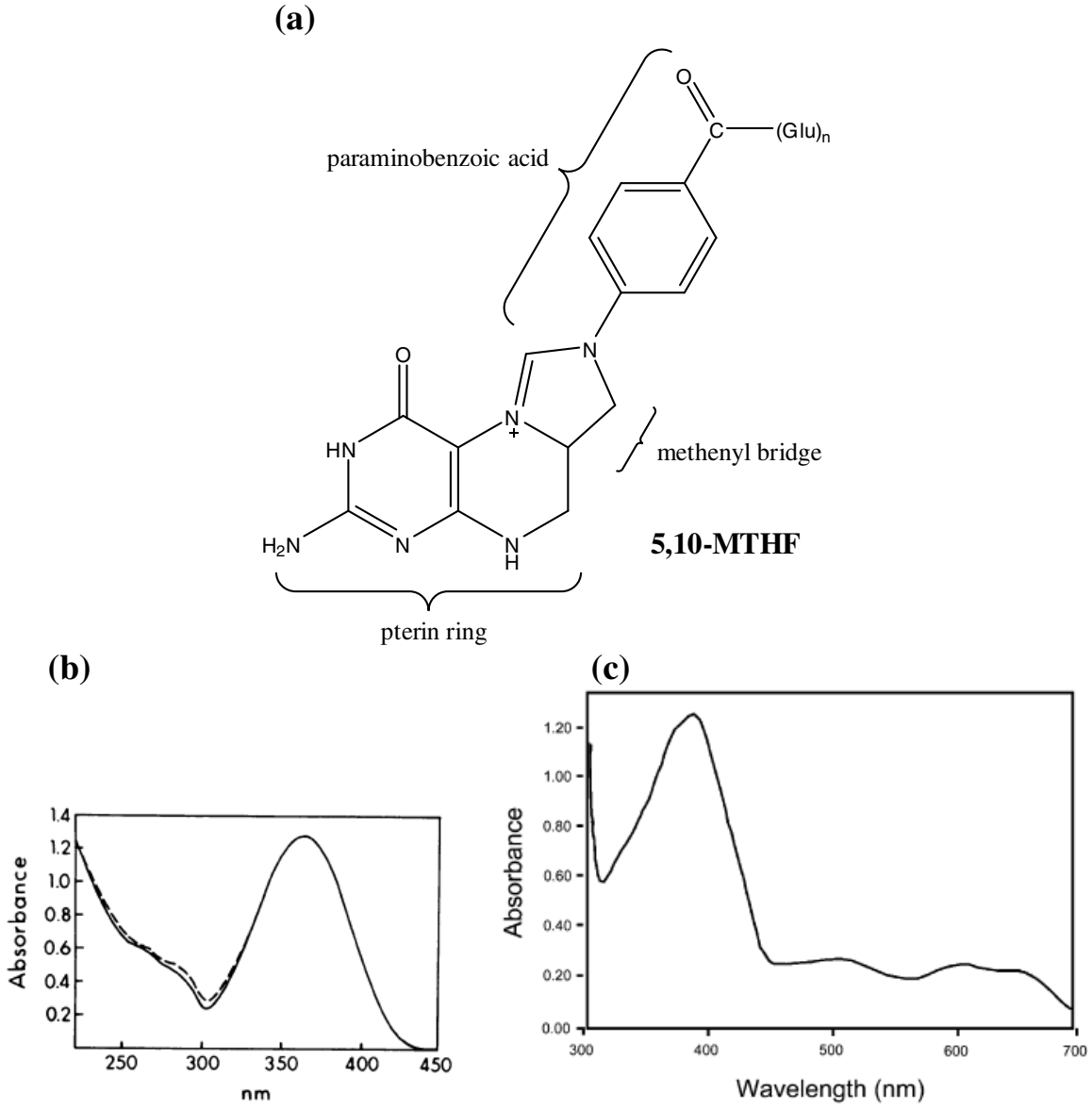

Figure 2. Chemical structure and absorption spectra of 5,10-MTHF. (a) Chemical structure of 5,10-MTHF. (b) Absorption spectrum of 5,10-MTHF that has been released and purified from *E. coli* photolyase (—) or has been chemically synthesized from 5-formyltetrahydrofolate (---) (9). The positively charged methenyl bridge causes the absorption maximum at 360 nm (9). (c) Absorption spectrum of native *E. coli* photolyase (1). The absorption of 5,10-MTHF bound to photolyase is red-shifted due to polar enzyme contacts with the positively charged methenyl bridge and hydrophobic interactions with the pterin ring (9). The absorption above 450 nm is from $FADH^{\circ}$.

ranges from three to six residues (9). The high extinction coefficient of MTHF (ε = 24,495 $M^{-1}cm^{-1}$) makes it an optimal photoantenna to absorb over 90% of the photons used for photoreactivation by photolyase (1,9).

Catalytic Chromophore – FAD

Flavins were first discovered in the 1930s with the discovery of riboflavin, the yellow pigment that is otherwise known as vitamin B2 (13). Since that discovery flavins have been identified in numerous other proteins and substances. Their essential role in many biological electron transfer processes is now well-established. Flavins are also important in other biological processes including soil detoxification, light production in bioluminescent bacteria, and both formation and reduction of oxidative stress (13).

Flavins exist in three primary forms: riboflavin, flavin mononucleotide (FMN), and flavin adenine dinucleotide (FAD). Riboflavin was named for its ribityl side chain (ribo) and the yellow color of the isoalloxazine ring system (flavin) (Fig. 3) (13). FMN was first discovered in a yeast yellow enzyme that catalyzes the oxidation of NADPH: an integral step to the process by which living cells convert food to energy (13). FMN differs from riboflavin with a phosphate group linked to the terminal hydroxyl group of the ribityl chain forming a phosphate-ester (Fig. 3) (13). FAD was discovered in D-amino acid oxidase and can be made by condensation of FMN and AMP to yield an adenosine bound to the terminal hydroxyl of the ribityl group (Fig. 3) (13). FAD is the form of flavin found most recently in the photolyase/cryptochrome family of photoreceptors.

The redox activity of flavin is carried out by the isoalloxazine ring system. There are three flavin redox states (Fig 4a) with distinct spectroscopic properties (Fig. 4b) (FAD in parentheses): fully reduced flavin ($FADH_2$) or ($FADH^-$), flavin semiquinone free radical

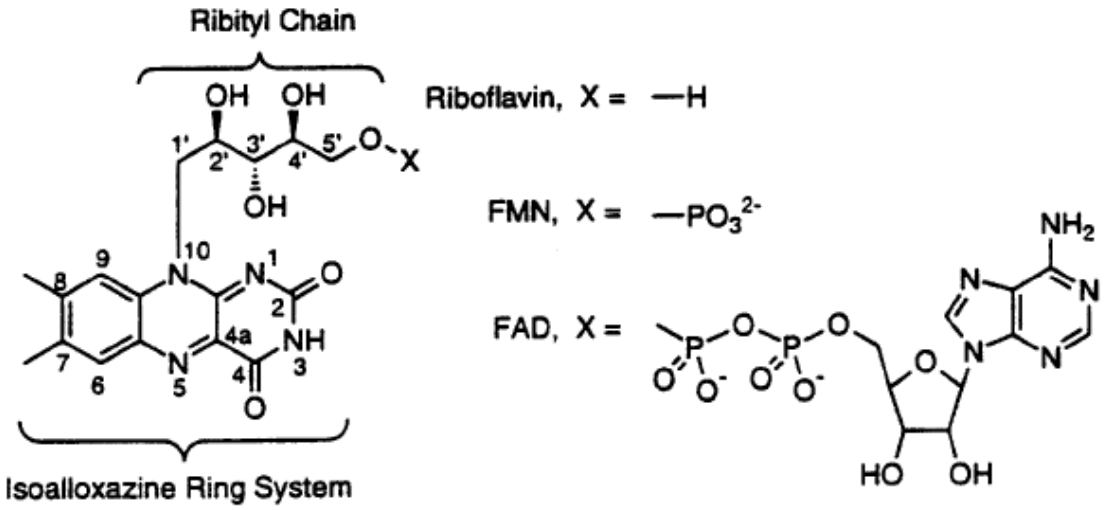

Figure 3. Forms of flavin. Flavin molecules consist of the redox reactive isoalloxazine ring system with a ribityl chain substituent on N-10. There are three primary forms of flavin that are found in nature: riboflavin, flavin mononucleotide (FMN), and flavin adenine dinucleotide (FAD), each of which differs in the substituent attached to the terminal hydroxyl group of the ribityl chain (13).

(a)

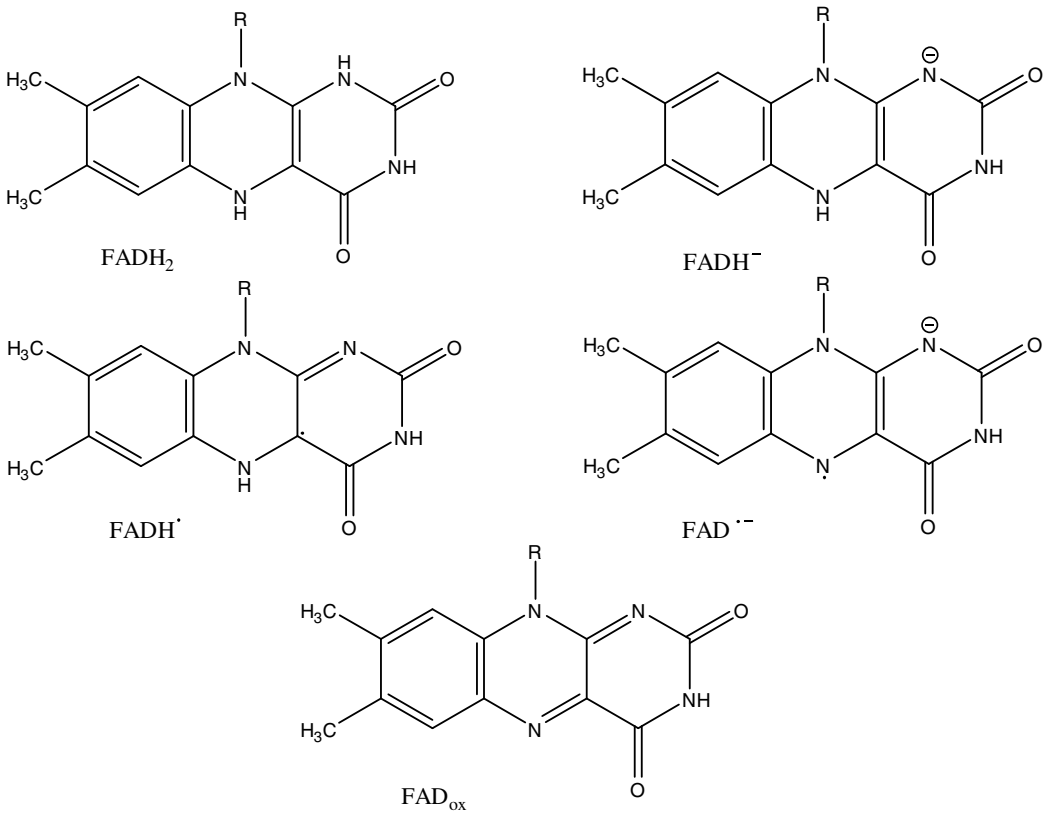

(b)

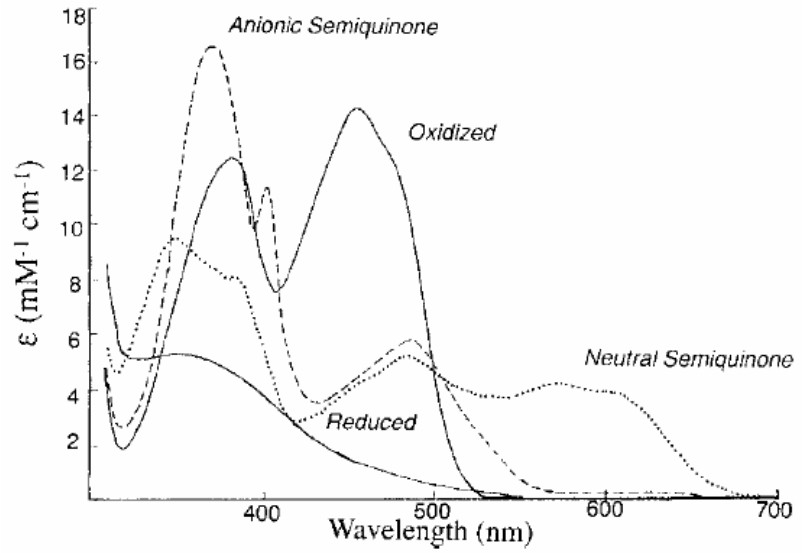

Figure 4. Flavin redox states and absorption spectra. (a) Chemical structures of the different flavin redox states: fully reduced neutral flavin ($FADH_2$), fully reduced anionic flavin ($FADH^-$), anionic semiquinone radical flavin ($FAD^{\circ-}$), neutral semiquinone blue-radical flavin ($FADH^{\circ}$), fully oxidized flavin (FAD_{ox}) (15). (b) There are four different absorption spectra for each distinct flavin redox state. Oxidized flavin (—) shows two primary peaks at 380 and 450 nm. The neutral semiquinone (···) shows absorption peaks at 360, 480, 580, and 620 nm. The anionic semiquinone (- - -) peaks at 380 and 480 nm with a small shoulder at 405 nm. The fully reduced flavin (—) shows very little absorption with a small shoulder at 360 nm (14).

($FAD^{\circ-}$) or ($FADH^{\circ}$), and oxidized flavin (FAD_{ox}) (13-15). The flavin semiquinone free radical typically exists in its anionic form ($FAD^{\circ-}$) or its neutral form ($FADH^{\circ}$), each of which can be detected by distinct absorption spectra (Fig. 4b). The catalytic role of FAD in photolyase (and possibly in cryptochrome) makes the study of its properties and physiological redox state and reactions crucial to an understanding of the enzyme's photocycle. The different spectroscopic properties of each flavin redox state (Fig 4b) conveniently make the spectroscopic study of this chromophore very useful (14). Spectroscopic laser technology has enabled the capture of excited $FADH^{-}$ transients and reaction intermediates to prove both electron transfer to and from a substrate and energy transfer between MTHF and $FADH^{-}$ in photolyase (16-17).

Photolyase mechanism

The photolyase photocycle has been well-characterized (Fig. 5). The enzyme binds to DNA and the damaged dinucleotide (i.e. Pyr<>Pyr) is flipped out into the active site of the enzyme. The MTHF photoantenna, located on the surface of the protein, captures a photon of light. Energy transfer between MTHF and the active form of catalytic flavin ($FADH^{-}$) creates the excited flavin molecule $(FADH^{-})^{*}$ which transfers an electron to the damaged DNA creating two radical species: neutral $FADH^{\circ}$ and $Pyr<>Pyr^{\circ-}$. The $Pyr<>Pry^{\circ-}$ spontaneously rearranges to yield two canonical pyrimidine bases. After the cleavage of the Pyr<>Pyr, back-electron transfer occurs to create the active $FADH^{-}$ to complete the cycle (3-5).

Energy transfer from MTHF to FADH was first shown by time-resolved fluorescence and absorption spectroscopy (18). Transient spectra of enzyme-MTHF-$FADH^{-}$, when compared to spectra of enzyme-MTHF, show more rapid MTHF* decay and appearance of

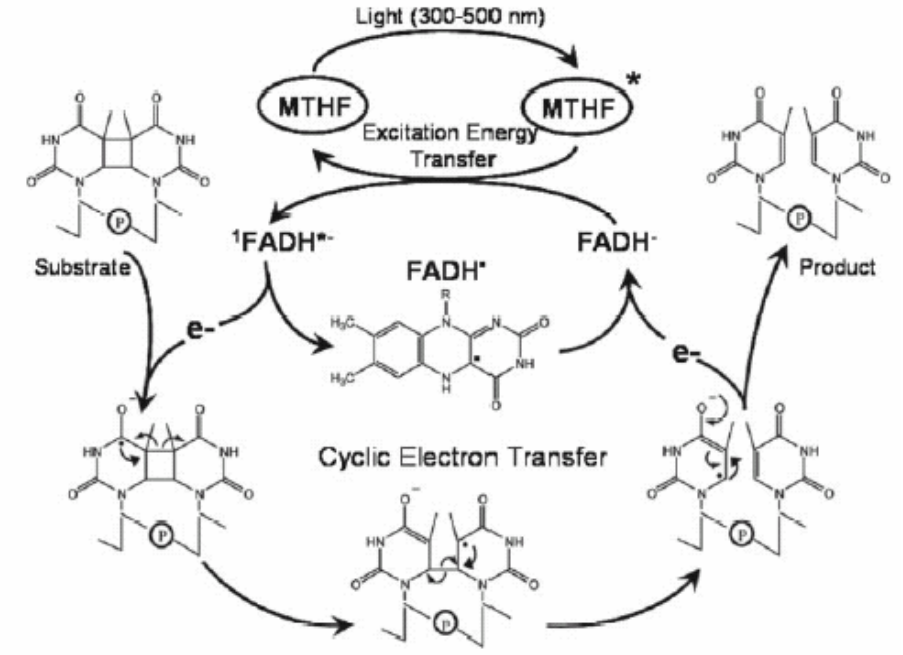

Figure 5. Photolyase photocycle. The reaction mechanism of photolyase is illustrated showing photon absorption by MTHF and electron transfer to $FADH^-$. Repair of the cyclobutane pyrimidine dimer occurs when the excited $FADH^-$* donates an electron forming two charge-separated radical species ($FADH^\circ$ and $Pyr<>Pyr^{\circ-}$). Splitting of the cyclobutane ring leads to restored catalytically active $FADH^-$ and repaired dinucleotide (4).

an absorption band at 500-600 nm; both of which provide direct evidence for energy transfer between the two cofactors (18). The dynamics of the electron transfer from the excited flavin molecule to the damaged DNA were studied to prove the radical mechanism. Since changes in redox state of the flavin cofactor occur faster than 1 ps, femtosecond-resolved absorption transients were used. Absorption transients were identified at two different wavelengths: 690 nm where only $FADH^{-}$* absorbs and 625 nm where both $FADH^{-}$* and $FADH^{\circ}$ absorb. The different decay kinetics at these two wavelengths provided direct evidence for electron transfer from the excited flavin cofactor to the damaged DNA that proceeds through a radical intermediate (16).

Cryptochrome phylogeny

There are two common forms of DNA damage and two types of photolyases that specifically repair each: cyclobutane pyrimidine dimer (CPD) photolyases and pyrimidine-pyrimidone photoproduct (6-4) photolyase (1). While photolyases are found in many prokaryotic species, they are absent in several eukaryotes including humans (19). Cryptochromes were discovered first in only plants and animals so it was originally thought they evolved from a photolyase progenitor. It was later shown that plant cryptochromes are more similar to CPD photolyases and animal cryptochromes are more similar to 6-4 photolyases supporting evolution of plant and animal cryptochromes from distinct photolyases (20). Questions were raised however, with the discovery of a new subset of proteins present in bacteria through vertebrates. They were originally classified as cryptochrome DASH proteins (named for four homologous cryptochromes from *Drosophila, Arabidopsis, Synechoystis*, and Human) because they possessed only marginal repair activity (21) and were not necessary for survival after UV exposure (22,23). Recently, cryptochrome

DASH proteins have been found to be single-stranded DNA specific photolyases and hence have been reclassified into the photolyase subfamily of the cryptochrome/photolyase family (24). The crystal structure of AtCry3, a member of this cryptochrome DASH subfamily, has revealed that the protein contains non-covalently bound MTHF and FAD which based on location and orientation maintain the redox potential that is found in CPD photolyases (25). However, it was also discovered that there are two amino acid substitutions and penetration of three charged residues into the CPD binding pocket which reduce the hydrophobicity of the pocket and thus decrease the affinity for the CPD lesion. In ssDNA, the decrease in affinity is of no consequence since there is no direct competition for binding of the CPD lesion. However, in dsDNA, the stacking and pairing interactions between the CPD lesion and the duplex DNA are more favorable than the interaction between the CPD lesion and the Cry-DASH protein (25). Therefore, the CPD lesion on dsDNA is not effectively "flipped-out" from the DNA backbone to bind to the Cry-DASH protein and thus cannot be efficiently repaired (25).

Human cryptochrome was the first animal cryptochrome identified (26) and shown to be an essential component of the molecular clock in mammals (27). However, the *Drosophila melanogaster* cryptochrome (dCry) which was identified later has been an excellent model by which to study the photochemistry of animal cryptochromes. Recently however, many insects have been found to possess two cryptochromes such as *Anopheles* (mosquito), *Bombyx* (silk moth), and *Danaus* (butterfly) similar to the two cryptochromes found in some basal animal lineages such as *Strongylocentrotus* (sea urchin). Of these two cryptochromes, one is similar to dCry whereas the other is similar to mouse cryptochrome 1 (mCry1) and other mammalian cryptochromes. It was also recently discovered that *Apis*

mellifera (honey bee) possess only one mCry-like cryptochrome (28). Additional components of the honey bee clock also more closely resemble that of mammals as opposed to *Drosophila*. These recent findings provide compelling evidence that the *Drosophila* clock may have actually diverged from the original basal insect lineage that included one *Drosophila*-like cryptochrome and one mammalian-like cryptochrome (28). Likewise, honey bee clocks likely converged evolutionarily with mammalian clocks to result in the loss of the *drosophila*-like cry (28).

Although it is increasing, the current knowledge fails to definitively identify the evolutionary relationship between photolyase and cryptochrome. Likewise the disconnect between the structural similarities but sequence and functional differences between photolyase and cryptochrome has yet to be fully explained. The characterization of cryptochromes from additional species will continue to contribute to the current body of knowledge and should bring us closer to a full understanding of the evolutionary relationship between these two classes of proteins.

Light-dependent in-vivo cryptochrome activity

Plant Cryptochromes

The first cryptochrome (AtCry1) was discovered in plants in 1993 as the protein encoded by the Hy4 gene of *Arabidopsis thaliana* when a genetic mutant caused loss of a photomorphogenic (growth and adaptation) response to high intensity blue-light (29). These mutants specifically suffered hypocotyl stem growth defects when grown in the dark (29). The protein's blue-light response, presence of flavin chromophore, and homology to photolyase all coupled with its lack of DNA repair activity created a novel class of blue-light photoreceptors named cryptochromes (30,31). A second *Arabidopsis* cryptochrome, AtCry2,

was identified later in 1996 that showed a photomorphogenic effect only under low light conditions (32,33). Later, AtCry2 was shown to specifically regulate photoperiodic flowering (34,35). Additionally, AtCry2 exhibited light-dependent degradation in normal to bright light conditions (33). AtCry1/AtCry2 double mutants resulted in a stronger phenotype than mutation of either cryptochrome alone, suggesting redundant roles with AtCry1 active in bright light conditions and AtCry2 active only in low light conditions (6). Additionally, many of the genes sensitive to blue-light in wild-type plants were also the same genes that were unresponsive to blue-light in the AtCry1/AtCry2 mutants, suggesting that AtCry1 and AtCry2 are the primary blue-light photoreceptors responsible for the observed blue-light photomorphogenic effect in *Arabidopsis* (36,37).

The light-dependent activity of AtCry1 and AtCry2 is thought to proceed primarily through regulation of gene expression. This has been shown to occur, at least in part, through direct protein-protein interaction with the E3 ubiquitin ligase COP1 (38). Light inhibits the ubiquitin ligase activity of COP1 (39) ultimately resulting in translocation of the protein out of the nucleus (40-42). COP1 has been shown to interact with both *Arabidopsis* cryptochromes independent of light (38,43). Overexpression of the cryptochrome C-terminal domain (CCT), however, resulted in a light-on phenotype or constitutive repression of transcription factors normally degraded by COP1 in the dark (38). Therefore, it was proposed that the photolyase homology region of cryptochrome is responsible for inhibition of the interaction between the CCT and COP1 in the dark (38). One of the most extensively studied transcription factors degraded by COP1 is a bZIP transcription factor, HY5, which binds to the promoters and induces the expression of light-inducible genes (44). Exposure to light prevents degradation of HY5 by COP1 and thus enables light-dependent

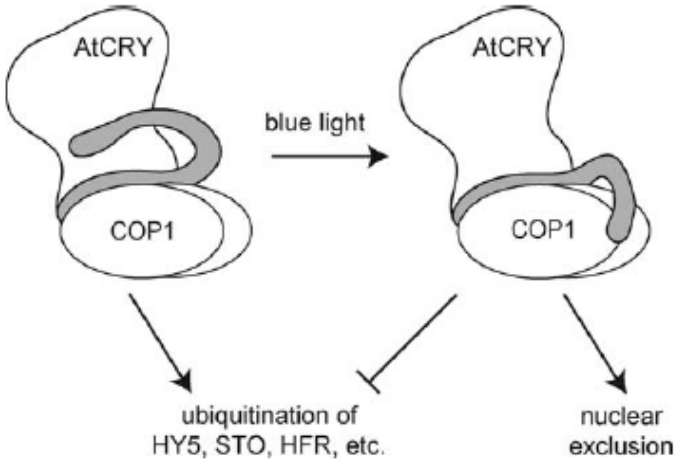

Figure 6. Model of *Arabidopsis* cryptochrome phototransduction pathway (6). Ubiquitin ligase 3 component, COP1, binds to AtCry1 in the dark while it actively ubiquitinates several targets including HY5, STO, and HFR. Exposure to blue-light induces a conformational change of the C-terminal tail of AtCry that inhibits the ubiquitin ligase activity of COP1 and leads to its nuclear exclusion (6).

photomorphogenic development of the plant (44). Other transcription factors, such as HFR1, are also degraded by COP1 and likely function in an analogous manner to HY5 (39). This model is illustrated in Figure 6 (6).

Animal Cryptochromes

Animal cryptochromes play an important role in synchronization of the central circadian clock with daily environmental light-dark cycles. Since most animals have an intrinsic circadian clock with a periodicity of either less than (*Drosophila* and mice) or more than (humans) 24 hours, synchronization with the 24-hr solar day is necessary. In general, circadian synchronization in animals is achieved through a non-visual (blue-light) photoreceptor in addition to classical visual photopigments including rods and cones (45-48).

Even though human cryptochrome was the first animal cryptochrome to be discovered as a circadian clock protein (26,27), the most extensively studied animal cryptochrome is the *Drosophila melanogaster* Cry (dCry) which, like the plant cryptochromes, has blue-light photoreceptor activity. dCry mutants demonstrate a slower clock oscillation pattern shift in response to light-dark cycling changes, absence of response to light pulses that would normally shift the circadian phase in wild type flies, and normal rhythm in continuous light conditions that causes arrhymicity in wild-type flies (49,50). dCry is a potent blue-light photoreceptor present in all tissues that is necessary for normal circadian periodicity; however, *Drosophila* only lose total light sensitivity when both dCry and the visual opsins are eliminated, suggesting some degree of redundancy between cryptochrome and opsins. Further study of Drosophila cryptochrome has revealed a light-independent interaction with an essential core clock protein, Timeless (TIM), modulated through a blue-light dependent conformational change of the 20 amino-acid C- terminal

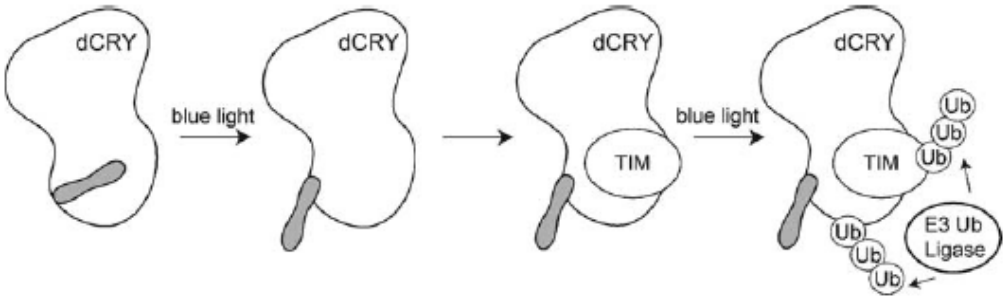

Figure 7. Model of *Drosophila* cryptochrome phototransduction pathway (6). Exposure to blue-light causes a conformational change of the 20 amino acid tail of dCry which enables the light-independent binding of TIM. Blue-light irradiation of TIM-bound dCry causes ubiquitin-mediated degradation of both TIM and dCry (6).

extension of dCry (51-53). Upon TIM binding to dCry, ubiquitin-mediated degradation of TIM and dCry, independent of the 20 amino acid C-terminal extension, occurs in response to blue-light exposure (51,54). The model for this phototransduction pathway of dCry is illustrated in Figure 7 (6)

Mammalian cryptochromes, unlike dCry, accomplish all photoreception through the retina with signal transduction to the suprachiasmatic nuclei (SCN) in the hypothalamus where the central clock machinery resides (4). When cryptochrome was first discovered in mammals it was thought to be the putative blue-light photoreceptor necessary for circadian entrainment (26). Further studies, however, have raised doubt that a photoreceptive function exists in mammalian cryptochromes. Mammalian cryptochromes have an additional light-independent transcriptional repressor function within the feedback loop of the clock (55,56) that renders behavioral activity of Cry knockout mice to be uninformative towards elucidating a photoreceptive role in mammalian cryptochromes (6). However, light-dependent induction of c-Fos by cryptochrome was lost significantly in Cry1-/-Cry2-/- double mutant mice lacking classical visual photoreceptors (57,58). The double knockout Cry mice, even in the presence of classical visual photoreceptors, showed 10- to 20-fold loss of c-Fos induction (57). Additionally, while cryptochrome in both *Drosophila* and mammals is present in all tissues, a mammalian circadian photoresponse can only occur through the eye, whereas *Drosophila* photoresponses occur through other organs (4). However, melanopsin, a novel blue-light opsin, was discovered recently and mice lacking classical opsins and melanopsin but not cryptochrome, lost all circadian photoreceptive activity (59,60). The current knowledge suggests mammalian cryptochromes likely have a role in the

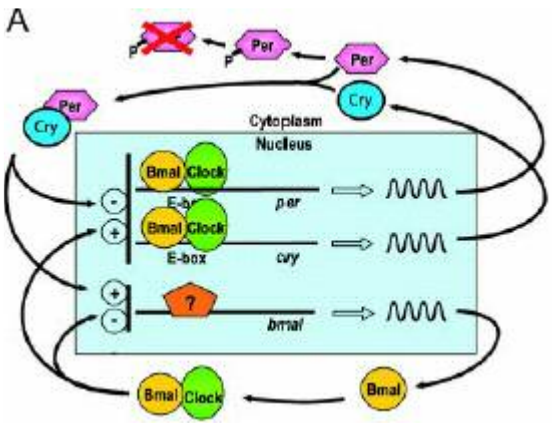

Figure 8. Mammalian circadian clock light-independent negative transcriptional feedback loop. Central clock *cry* and *per* genes are transcriptionally activated by Bmal1/Clock (yellow/green) heterodimer binding to an E-box promoter. Cry and Per proteins then form a heterodimer that translocates to the nucleus where it disrupts Bmal1/Clock-dependent transcriptional activation of *cry* and *per* genes. Subsequent decrease in Cry and Per levels re-activates Bmal1/Clock stimulated transcription to complete the feedback loop (4).

circadian phototransduction pathway, but that they are neither essential nor sufficient as the putative blue-light photoreceptors of this pathway (6).

Light-independent cryptochrome activity

Mammalian cryptochromes demonstrate a light-independent transcriptional repressor activity that engenders a negative feedback loop in the circadian clock mechanism (Fig. 8). Transcription of the central clock genes, *per* and *cry*, are activated by binding of the transcription factor heterodimer, Clock/Bmal1, to an E-box element in their promoters. Cry and Per proteins form a heterodimer that translocates to the nucleus where they disrupt Bmal1/Clock activity through an ill-defined mechanism, which subsequently reduces *per* and *cry* transcription. Reduced Cry and Per protein levels lead to reactivated Bmal1/Clock stimulated transcription of *per* and *cry* genes creating the transcriptional feedback loop (4).

Recently, an analogous transcriptional loop has also been observed in *Drosophila* where dCry appears to possess a light-independent transcriptional repressor activity in the peripheral clocks of *Drosophila* in addition to its photoreceptive function detailed above (61). In *Drosophila*, the Clock/Cycle transcription factor heterodimer activates transcription of the *per* and *tim* genes. As in mammals, the resulting proteins, Per and Tim, dimerize and enter the nucleus to inhibit Clock/Cycle gene activation (61).

Danaus plexippus cryptochromes

Recently, two cryptochromes have been identified in the monarch butterfly, *Danaus plexippus*: DpCry1 which shows moderate sequence homology to dCry (62), and DpCry2 which shows higher sequence homology to mammalian cryptochromes than to DpCry1 (63). Reppert and colleagues (63) assessed the relative *in vivo* photosensitive and transcriptional repressor activities of these proteins with expression in *Drosophila* Schneider 2 cells.

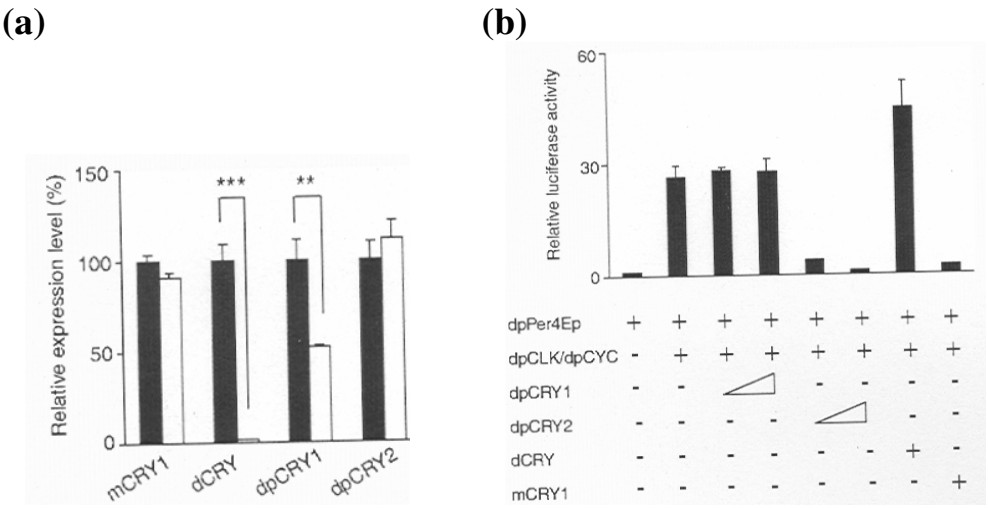

Figure 9. **DpCry1 undergoes photodegradation and DpCry2 functions primarily as a transcriptional repressor.** (a) DpCry1 undergoes photodegradation but DpCry2 does not. *Drosophila* Schneider 2 (S2) cells were co-expressed with V5 β-galactosidase and V5-tagged mCry1, dCry, dpCry1, or dpCry2. Cells were exposed to 6 hrs of dark (black bars) or light (white bars) and cry protein levels in cell extracts were measured and quantified by western blot analysis (anti-V5) and densitometry respectively. The dark values were normalized to 100% (63). (b) DpCry2 functions primarily as a transcriptional repressor but DpCry1 does not. A luciferase reporter gene containing an E-box per gene promoter (dpPer4Ep) was transfected into S2 cells and the activity was measured in the presence and absence of the butterfly transcriptional activator heterodimer, dpCLK/dpCYC (orthologs of mammalian Bmal1/Clock). dpCry1, dpCry2, dCry, or mCry1 were co-transfected in the presence of dpCLK/dpCYC to assess transcriptional repression measured by relative luciferase activity (63).

DpCry1 was degraded in response to light analogous to dCry but both mCry1 and DpCry2 showed no degradation (Fig. 9a) (63). Additionally, both DpCry2 and mCry1 demonstrated transcriptional repression of a luciferase reporter gene containing an E-box and a period gene promoter while DpCry1 and dCry did not (Fig. 9b) (63). Based on this data, I hypothesized that DpCry1 may have biochemical properties to support light-dependent photoreceptor activity and that DpCry2 will have biochemical properties similar to those of other mammalian cryptochromes.

Biochemical properties of cryptochrome

Spectroscopic properties

Purification of recombinant flavoproteins such as those in the photolyase/cryptochrome family of blue-light photoreceptors often leads to loss of chromophores during purification and/or chromophore oxidation. For this reason, flavin composition and redox state in recombinant flavoproteins must be supplemented with supporting data to conclude the chromophore composition and redox state of the flavin *in vivo*. Purification of photolyase from several species has regularly yielded near-stoichiometric levels of flavin supporting the conclusion that photolyase contains stoichiometric flavin *in vivo* (64). Identification of the photolyase photocycle and the crucial role of flavin in this mechanism further support this conclusion. *Arabidopsis* cryptochrome (AtCry1,AtCry2), which are known to function as photoreceptors, have been purified with near-stoichiometric catalytic flavin (Fig. 10b) (30,65). The recombinant dCry photoreceptor, however, contains less than 5% flavin, an apparent contradiction to its known photoreceptive function (Fig. 10c) (1,66,67). However, since flavin can often be lost after overexpression in

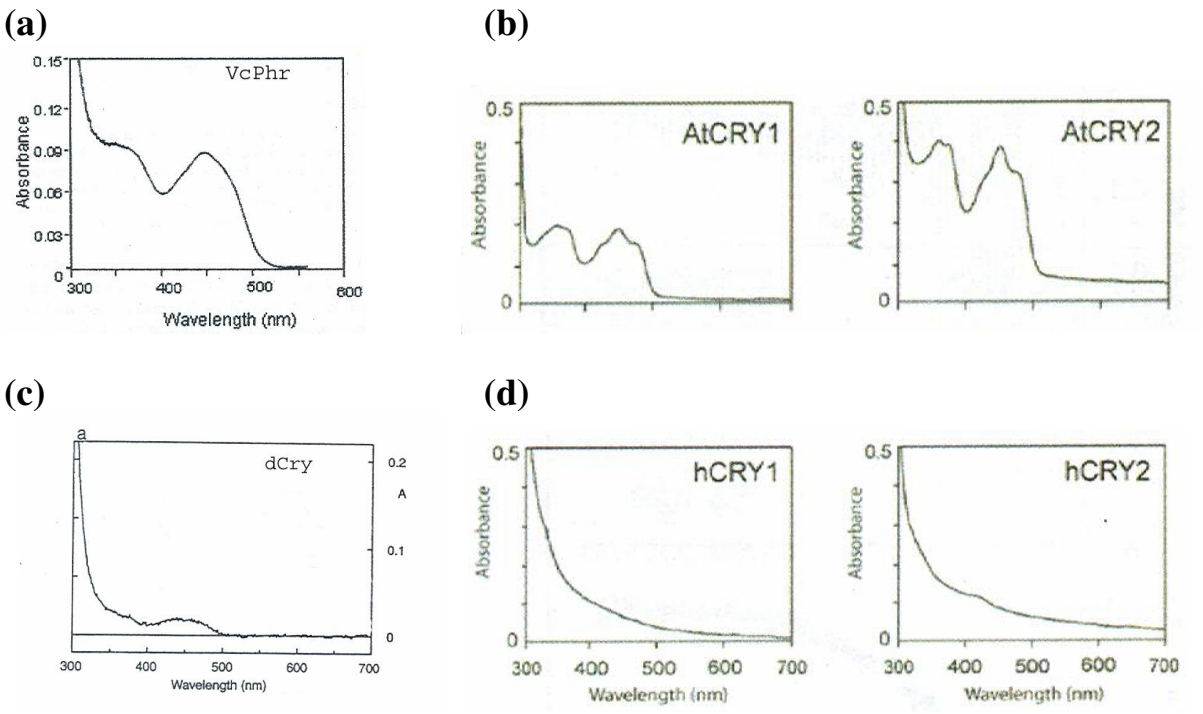

Figure 10. Absorption spectra of proteins from the photolyase/cryptochrome family (64). (a) Heat-denatured VcPhr absorption spectrum shows stoichiometric levels of flavin as evidenced by the presence of FAD_{ox} absorption at 440 nm (23). (b) AtCry1 and AtCry2 native protein spectra show stoichiometric levels of flavin as shown by FAD_{ox} absorption peaks at 370 and 440 nm (65). (c) Heat-denatured dCry absorption spectrum shows less than 5% flavin (67). (d) hCry1 and hCry2 native protein absorption spectra show very little flavin (65).

heterologous systems as well as during purification, the fact that recombinant dCry lacks flavin does not mean that it doesn't exist *in vivo*. Recombinant human cryptochromes (hCry1, hCry2) have been purified with less than 2% flavin (Fig. 10d), but a light-dependent mechanism for these and other mammalian cryptochromes has yet to be identified (26). In light of the recent hypothesis that dCry may actually have diverged from a basal insect lineage that included a *Drosophila*-like and mammalian-like cryptochrome, it is beneficial to study the spectroscopic properties of cryptochromes from an insect that contains both types such as *Danaus plexippus* (monarch butterfly). Therefore, I purified insect-like DpCry1 and mammalian-like DpCry2 from a bacterial expression system using low-stringency purification conditions in order to retain their chromophores and study their biochemical properties. I spectroscopically characterized the insect-like DpCry1 and mammalian-like DpCry2 proteins to better understand properties of cryptochromes with distinct light responsiveness. These experiments will be discussed in chapter 2.

Autophosphorylating kinase activity of cryptochrome

Phosphorylation has been found to contribute to regulatory processes of many photoactive enzymes. Phosphorylation activity of cryptochromes, however has not been extensively studied and the current data are contradictory. The most heavily studied cryptochrome kinase activity is that of *Arabidopsis* Cry1 and Cry2; both of which play important roles in light-stimulated photomorphogenic responses in plants and have been purified with near-stoichiometric levels of flavin. *In vivo*, AtCry2 has shown blue-light dependent phosphorylation directly connected to its regulatory function, however, the identification of this activity as autophosphorylation has not been directly tested (68). More recently, AtCry1 was reported to have blue-light-stimulated kinase activity both *in vivo* and

in vitro (69). The activity was also shown to be dependent on both the presence of flavin and its redox state (69). Additionally, AtCry1 has shown stoichiometric ATP binding within the active site of the enzyme (8,70). Both autophosphorylation and ATP binding were shown for hCry1 as well, however flavin dependence was not tested since human cryptochromes have yet to be purified with greater than trace amounts of flavin (70).

The most recent data however show equal levels of light-independent autokinase activity in both human cryptochromes and in AtCry1 (65). Contrary to earlier reports, this activity in AtCry1 was shown to be independent of light and the redox state of flavin (65). Additionally, AtCry2 showed no autophosphorylation activity at all (65). Interestingly, human Cry1 and Cry2, which contain no flavin, exhibited similar levels of autokinase activity when compared to AtCry1 (65). These latest findings raise some questions as to the physiological relevance of autophosphorylation activity as well as its response to light and both the presence and redox state of flavin. There is clearly more work to be done to determine the role and importance of this autophosphorylation activity in cryptochromes. Since this activity has not been tested in any insect-like cryptochromes, I tested both recombinant DpCry1 and DpCry2 for autophosphorylation activity in a dark environment and these results will be discussed in chapter 2.

Photophysical Cryptochrome Properties

As mentioned previously, absorption transients of excited flavin have been isolated in photolyase (16). In photolyase, this technology has proven the long-predicted radical mechanism of photoreactivation (16). Excited flavin ($FADH^{-}$*) absorption, in the presence of T<>T substrate, was measured at 690 nm between 0.05 ns and 2.8 ns after excitation to observe the decay rate of the excited flavin ($FADH^{-}$*) (Fig. 11b). At this high wavelength,

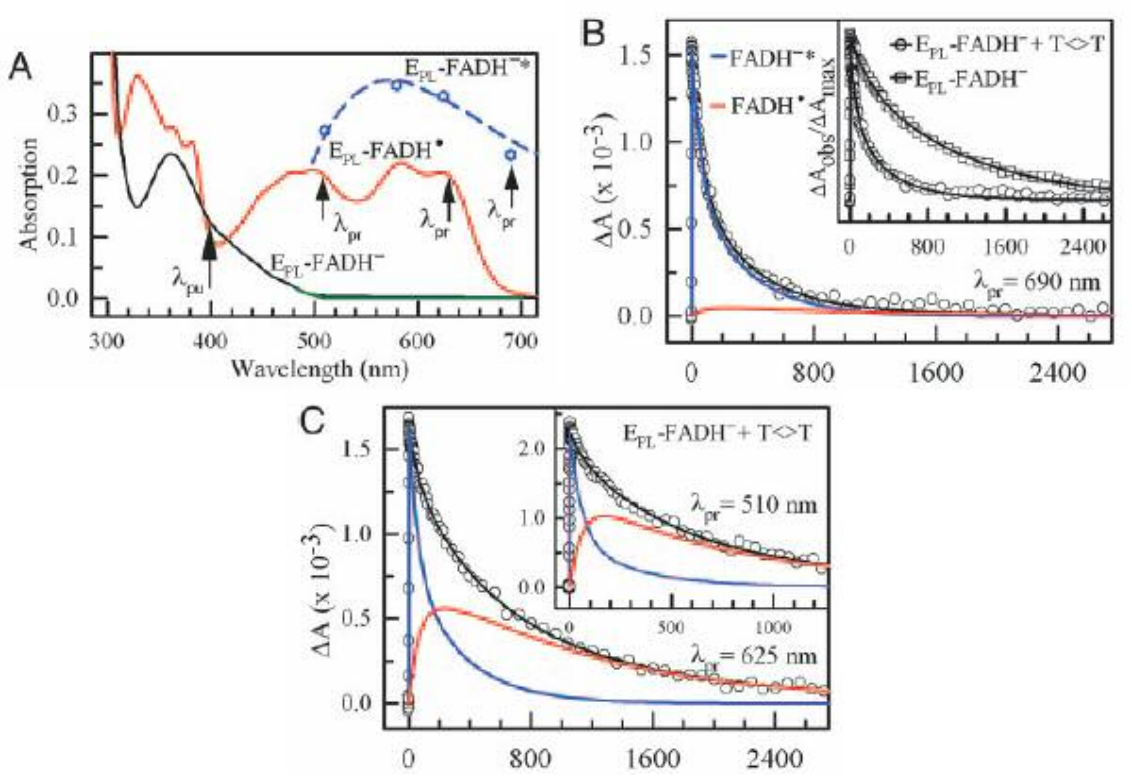

Figure 11. Photophysical dynamics of *E. coli* photolyase electron transfer from flavin to DNA damage. (a) The absorption spectra of the different flavin redox states: reduced flavin (—), neutral blue-radical flavin (—), and excited flavin (---) The black arrows depict wavelengths at which absorption transients were collected. (b) Absorption transient (○) collected in the presence of T<>T substrate at 690 nm: excited flavin (—), neutral blue-radical flavin (—). The inset shows the difference between transient decay at 690 nm in the presence (○) and absence (□) of T<>T substrate. In the absence of T<>T, the transient lifetime represents the lifetime of $FADH^{-}$* independent of any electron transfer to DNA. (c) Absorption transient (○) collected in the presence of T<>T substrate at 625 nm and 510 nm (inset). The transient decay curve at 690 nm represents $FADH^{-}$* decay (—) and the difference between the two curves shows formation of $FADH^{\circ}$ (—) (16).

the only absorbing species is $FADH^{-}$* (Fig. 11a). However, at shorter wavelengths above 500 nm both $FADH^{-}$* and the neutral radical ($FADH^{\circ}$) absorb. Therefore the difference between the $FADH^{-}$* decay curve at 690 nm and those recorded at either 625 nm or 510 nm can be attributed to formation of $FADH^{\circ}$ (Fig. 11c) (16).

Since there is no known substrate for cryptochromes, identification of reaction intermediates is not possible at this time. However, our collaborator, Dr. Dongping Zhong (Ohio State University), has successfully assessed the resonance energy transfer dynamics between MTHF* and $FADH^{-}$ of VcCry1 (17). If no energy transfer exists between the excited folate and flavin, the MTHF* transient decay should resemble a single exponential decay curve with a lifetime representative of that of free MTHF and any change in flavin redox state would have no affect on the lifetime. When MTHF* transient decay was tested, however, it was best fitted using three different exponential components each with a different lifetime: 10 ps, 60 ps, and 845 ps (Fig. 12) (17). The relative contribution of each component to the lifetime curve drastically changed when the majority of the $FADH^{-}$ was oxidized to FAD_{ox} (17). These two facts together prove the existence of energy transfer between MTHF and $FADH^{-}$ in VcCry1. It has recently been shown that VcCry1 is actually a single-stranded DNA specific photolyase and not a bona fide cryptochrome (24) and therefore the photophysical dynamics of cryptochromes have never been studied. Careful purification of DpCry1 to retain its chromophores enabled the use of this technology to analyze, for the first time, the photophysical dynamics of DpCry1 and these results will be discussed in chapter 2.

Conclusions

In conclusion, I purified and analyzed the biochemical properties of insect-like DpCry1 and mammalian-like DpCry2 in an effort to extend the knowledge of the specific

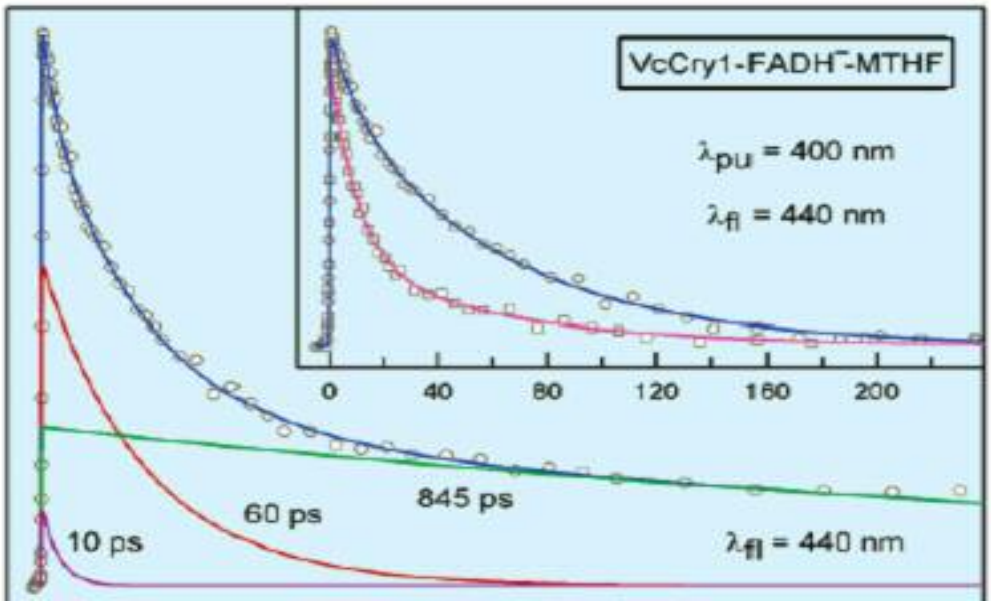

Figure 12. Fluorescence transients of MTHF* in VcCry1 (42). The fluorescence transient of excited folate (○) at 440 nm can be fitted to three separate exponentials with different lifetimes: 845 ps (—) representing the lifetime of free MTHF*, 60 ps (—) representing the energy transfer from MTHF* to $FADH^-$, 10 ps (—) representing the energy transfer from MTHF* to FAD_{ox}. The inset shows the faster decay with VcCry1 containing mostly FAD_{ox} (□). This decay curve could be fitted to the same exponentials but with different amplitudes; making it possible to identify the source of each component (17).

biochemical properties of cryptochromes that appear to possess differential responsiveness to light. An important step towards elucidating the photoreactive mechanism and phototransduction pathways of cryptochrome is to clearly understand the biochemical properties of a cryptochrome photoreceptor. Comparison of active cryptochrome photoreceptors such as dCry and DpCry1 with cryptochromes that apparently lack light-dependent activity such as hCry1, hCry2, and DpCry2 will bring us closer to this goal. The identification of the blue-light photocycle of cryptochrome will be crucial towards a global understanding of circadian rhythms; inevitably bringing us closer to understanding the link between circadian disruption and health disorders including cancer.

CHAPTER 2

PURIFICATION AND CHARACTERIZATION OF DPCRY1 AND DPCRY2

Materials and Methods

Cloning of D. plexippus Cryptochromes

The *D. plexippus* cryptochrome genes were amplified by PCR using primers designed from the published sequences (62,63) and pAC5.1 DpCry1 and pCR-BluntII-TOPO DpCry2 expression plasmids donated by Dr. Steven Reppert (University of Massachusetts, Worcester, MA) (62,63). The amplified genes were inserted into pMal-c2 bacterial expression vector (New England Biolabs). The plasmids each encode a *D. plexippus* cryptochrome protein fused to the C-terminus of maltose-binding protein (MBP) which is transcribed from the malE gene within pMal-c2. The cloned plasmids were named pDpCry1 and pDpCry2 which encode for MBP-DpCry1 and MBP-DpCry2 respectively. A C-terminal truncation mutant of DpCry2 (DpCry2tr) missing the last 573 base pairs (bp) of the full length gene was also cloned in the same manner using a different reverse primer to encode for the truncated mutant. The DpCry1 and DpCry2 genes are illustrated in Figure 13.

Protein Expression and Purification

Purification was carried out using standard MBP-fusion protein purification protocols as described by the manufacturer (New England Biolabs). Purification of MBP-DpCry1, MBP-DpCry2, and MBP-DpCry2tr was initiated with transformation of pDpCry1, pDpCry2,

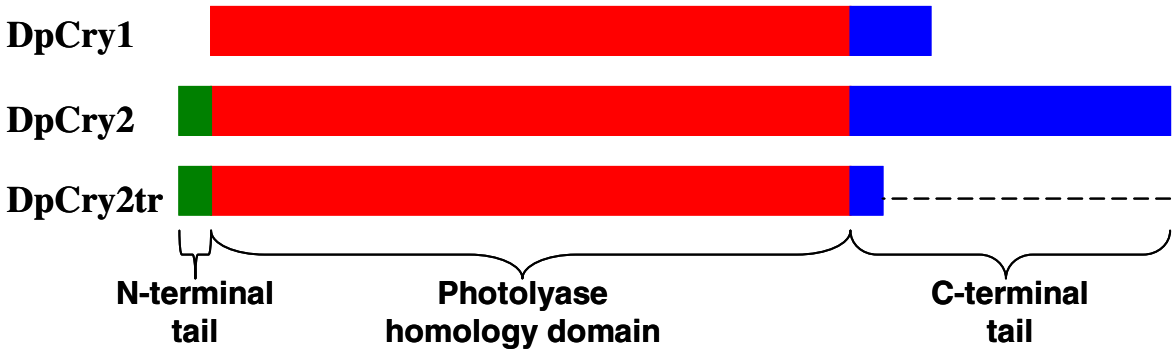

Figure 13. Genetic maps of the *Danaus plexippus* cryptochromes. DpCry1 (top) possesses a photolyase homology domain with a short, 186 bp, C-terminal extension. DpCry2 (middle) also contains a photolyase homology domain with a short N-terminal tail and a longer, 708 bp, C-terminal tail. A truncated DpCry2 (bottom) lacking the last 573 bp was also cloned and purified using a different reverse primer.

and pDpCry2tr, respectively, into BL21-codonplus (DE3)-RIPL competent *E. coli* cells (Stratagene). All three strains were grown in luria broth (LB) at 37ºC to A_{600}=0.5. Gene induction with 0.1 mM Isopropyl-1-thio-β-galactosidase (IPTG) was carried out at 15 ºC for 16 hrs. Bacteria were harvested by centrifugation and the cell pellets frozen on dry ice, thawed, and resuspended in column buffer (CB) containing 20 mM Tris-HCl pH 7.4, 200 mM NaCl, 1 mM EDTA, 10 mM β-mercaptoethanol, and 0.5 mM phenylmethylsulfonyl fluoride (PMSF). Cell free extract was prepared by addition of chicken egg lysozyme (Invitrogen) to 10 mg/mL, one freeze/thaw using dry ice to freeze and warm water to thaw, and sonication (10 x 10 s) followed by ultracentrifugation at 35,000 rpm in a Beckman L-80 centrifuge with a Ti45 rotor at 4ºC for 1.5 hr to remove insoluble material. Cell free extract was loaded onto a 20 mL amylose resin column (pre-equilibrated with 200 mL CB) at a flow-rate of 1 mL/min. A limited (120 mL) and low-salt wash was conducted with CB and elution of proteins was performed using 32 mL of a moderately high salt elution buffer (EB) containing 50 mM Tris-HCl pH 7.4, 300 mM NaCl, 1 mM EDTA, 5 mM dithiothreitol, 10% (v/v) glycerol, 0.5 mM PMSF, and 15 mM maltose. Elution fractions containing protein were identified by SDS-PAGE and Coomassie-Blue staining and the most highly concentrated fractions were combined and concentrated (Vivaspin 20, 30,000 MWCO) by centrifugation at 5,000 rpm in a Sorvall RC 5B Plus centrifuge until the total volume was between 750 μL and 1 mL. Proteins were dialyzed into storage buffer (SB) containing 50 mM Tris-HCl pH 7.4, 100 mM NaCl, 1 mM EDTA, 5 mM dithiothreitol, and 50% (v/v) glycerol for 24 hrs at 4°C. Final protein concentration was quantified by SDS-PAGE and Coomassie-Blue staining against a bovine serum albumin (BSA) standard. Typical yield

from 12 L of cells was approximately 2 mg (50 μM in 400 μL) of MBP-DpCry1, 3 mg (60 μM in 400 μL) of MBP-DpCry2, and 6 mg (91 μM in 600 μL) of MBP-DpCry2tr.

Spectroscopic Analysis

Absorption and fluorescence spectra were obtained using a Shimadzu UV-601 spectrophotometer and a Shimadzu RF5000 U spectrofluorometer, respectively. Native protein absorption spectra were recorded between 300 and 700 nm for all purified proteins. MBP-DpCry1 was heat-denatured (95ºC, 10 min), centrifuged at 13,000 rpm (VWR Galaxy 14D) for 15 min to remove denatured protein, and its absorption at 440 nm recorded to obtain the concentration of the flavin content of the protein (23). The molar extinction coefficient of flavin at 440 nm, 11,300 $M^{-1}cm^{-1}$, was used to calculate flavin concentration which ranged between 30-60 μM leading to flavin:protein ratios that ranged from 0.7–1.0. Since flavin levels in MBP-DpCry2 and MBP-DpCry2tr were too low to be detected by absorption, its concentration in these proteins was determined using fluorescence spectroscopy. Direct comparison of the fluorescence of a heat-denatured (95ºC, 10 min) 1:5 dilution of protein to a flavin standard curve enabled me to accurately determine the flavin concentration in each protein. MBP-DpCry2 flavin concentration was approximately 3 μM leading to a flavin:protein ratio less than 0.05. MBP-DpCry2tr flavin concentration was approximately 4 μM leading to a flavin:protein ratio also less than 0.05. Verification of flavin content of each protein was accomplished by fluorescence spectroscopy after heat-denaturation of a 1:5 protein dilution at pH 2 containing 0.7% SDS. Emission spectra for excitation at 440 nm and excitation spectra for emission at 520 nm were recorded to verify the presence of flavin. The MTHF content in each protein was qualitatively assessed by fluorescence emission of native protein at 460 nm after excitation at 400 nm (23).

Kinase Assay

Autophosphorylation activity was tested as described previously (65,69) in a 20 μL reaction contained 50 mM Tris-HCl pH 7.4, 5 mM $MgCl_2$, 50 μM ATP [plus 5 μCi of γ-^{32}P-ATP (4500 Ci/mmol)], and 10 mM βME. Each reaction contained comparable levels of DpCry1, DpCry2, and AtCry1. The reaction was incubated at 23ºC for 1 hr under "Gold" fluorescent light to avoid any uncontrolled blue-light dependent autophosphorylation activity (dark conditions). The reaction was stopped by addition of 2X SDS-PAGE loading dye (0.125 M Tris-HCl, pH 6.8, 4% SDS, 20% glycerol, 10% βME, 0.5% bromophenol blue) and boiling at 95ºC for 10 min. Proteins were separated by SDS-PAGE and analyzed by Coomassie-Blue staining. Protein phosphorylation was assessed by γ-^{32}P-ATP incorporation and visualized by phosphorimaging.

Photophysical Analysis of DpCry1

The fluorescence lifetime of flavin in DpCry1 was analyzed using a femtosecond-resolved fluorescence up-conversion technique using a 400 nm laser pulse of 50 fs and monitoring emission at 550 nm (71).

Results and Discussion

Protein Purification

DpCry1 and DpCry2 genes were obtained from Dr. Reppert and colleagues and cloned into the pMal-c2 expression vector to express MBP fusion proteins. MBP fusion was used to increase protein overexpression and solubility. MBP-DpCry1 (104 kDa) (Fig. 14a) and MBP-DpCry2 (127 kDa) (Fig. 14b) were highly overexpressed in BL21 *E. coli* cells and purified by affinity chromatography on an amylose resin column and analyzed by SDS-PAGE. While initial overexpression attempts at room temperature led to large amounts of insoluble DpCry2, 16 hr gene induction using 0.1 mM IPTG at 15ºC resulted in nearly 50% soluble MBP-DpCry1 and MBP-DpCry2 for further purification (Fig. 14a, 14b). Purification was carried out using the standard MBP-fusion protein purification protocols as described by the manufacturer (New England Biolabs) with limited washing (6 column volumes) in low-salt column buffer that was used to help retain the chromophores and a higher-salt maltose-containing elution that was used to increase protein recovery during the concentration of each protein. These modifications led to final purity for both proteins of approximately 50% (Fig. 14a-b, lane 5). Primary contaminants in the purifications of MBP-DpCry1 and MBP-DpCry2 consist of free MBP (43 kDa) and a 60-70 kDa species which is likely either a cleavage product of the MBP-cryptochrome or a 60-70 kDa heat-shock protein that often purifies with proteins containing unstructured regions similar to the C-terminal extension of cryptochromes. However, neither 100% purity nor identification of the contaminants is essential for the spectroscopic analyses conducted on each protein. As a control, free MBP was overexpressed and purified using identical conditions as described above (Fig. 14d). MBP-DpCry1 and MBP-DpCry2 were concentrated and dialyzed into 50%

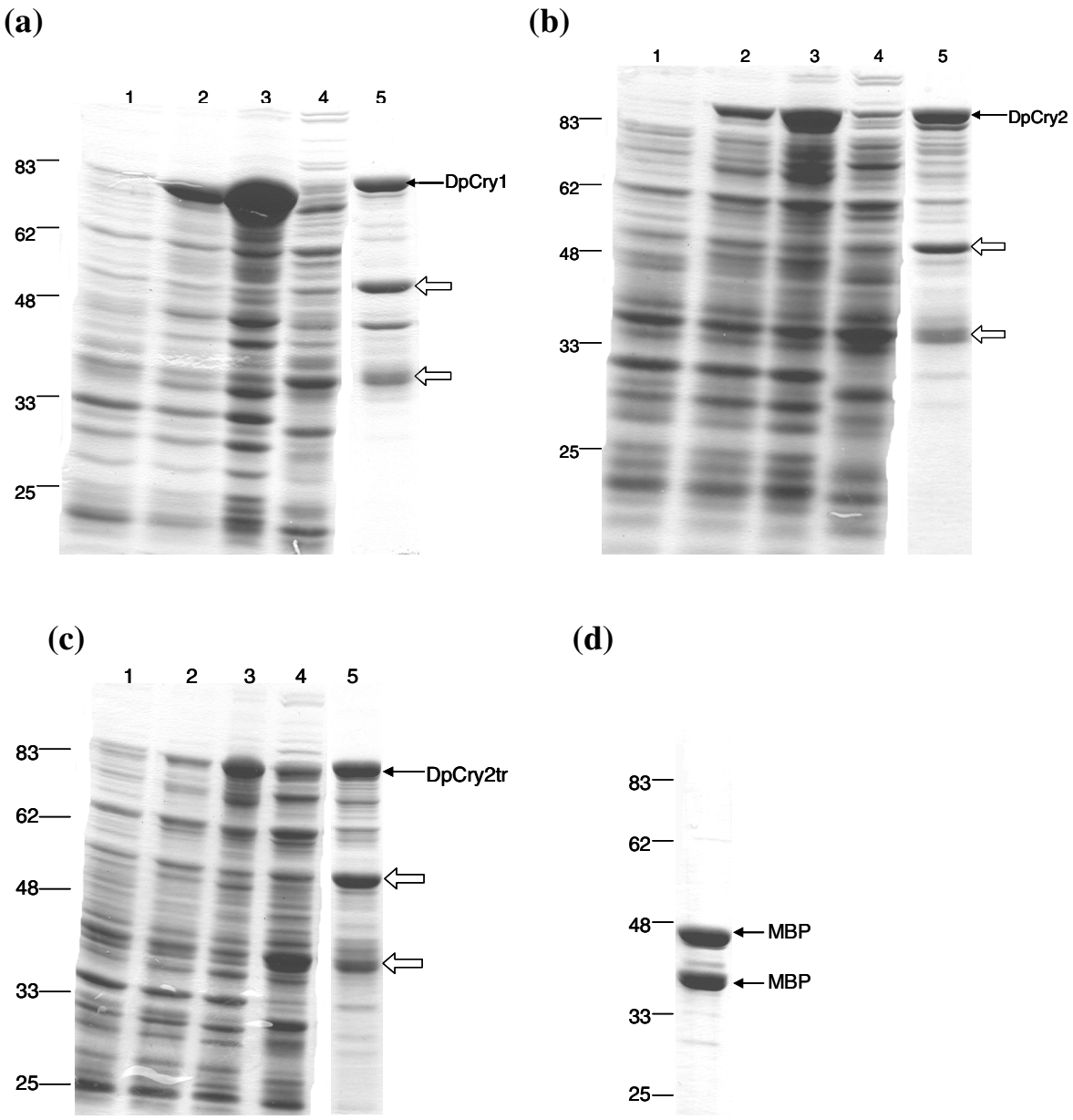

Fig 14. Purification of *D. plexippus* cryptochromes. Overexpression and purification of (a) DpCry1 (104 kDa), (b) DpCry2 (127 kDa), and (c) DpCry2tr (106 kDa). Protein fractions were analyzed by 10% SDS-PAGE and Coomassie Blue staining. Lane 1: 300 μL uninduced cells, lane 2: 300 μL of IPTG-induced cells, lane 3: insoluble fraction after lysis (8 μL), lane 4: cell free extract (10 μL), lane 5: purified protein before concentration and dialysis (20 μL). Free MBP (43 kDa) and a 60-70 kDa heat shock protein (indicated by open arrows) are the primary contaminants after purification. All proteins migrated faster than expected from their theoretical molecular weights. (d) Purification of MBP (43 kDa) used as a control for spectroscopic analyses. Free MBP resolves as two distinct species.

glycerol in storage buffer typically to a final concentration of about 50 μM and 60 μM respectively as determined by SDS-PAGE Coomassie-blue staining against a BSA standard.

A DpCry2 truncation mutant lacking the last 191 amino acids at the C-terminus of the protein (DpCry2tr) was purified as described above (Fig. 14c). This point of truncation was chosen based on a previously published AtCry1 C-terminal truncation mutant that contained the entire photolyase-homology region and flavin binding site (30). Sequence alignment of DpCry2 with AtCry1 enabled generation of an analogous DpCry2 C-terminal truncation mutant. This mutant was constructed and purified to increase the potential for chromophore retention in DpCry2, as was done previously with *Arabidopsis thaliana* cryptochrome 1 (30).

Spectroscopic Characterization of DpCry1

All cryptochromes characterized to date possess some amount of the essential flavin chromophore as well as varying amounts of MTHF. MTHF (with some contribution from FAD_{ox}) exhibits a distinct peak at 370-380 nm while FAD_{ox} has an additional peak at 450 nm. However, the presence of any neutral blue-radical flavin ($FADH^{\circ}$) gives rise to several additional absorption maxima at 480, 580, and 625 nm. Most characterized cryptochromes contain FAD_{ox}, $FADH^{\circ}$, or a mixture of the two (1). The native absorption spectrum of DpCry1, however, very convincingly suggests the presence of the anionic radical form of flavin ($FAD^{\circ-}$) with a large peak at 380 nm, a small shoulder at 405 nm, and a smaller peak at 470 nm (Fig. 15a) (13,15). There is a small amount of oxidized flavin (FAD_{ox}) as shown by the small peak around 450 nm. There is no evidence of MTHF from the absorption spectrum of native DpCry1 based on the relative magnitude of the absorption maximum at 370 nm (where MTHF absorbs) in DpCry1 that is nearly identical to the absorption maximum at 370 nm for the theoretical spectrum of $FAD^{\circ-}$ (Fig. 4b). To determine the

initial dark-state of flavin in DpCry1, the protein was purified under dark conditions and the absorption recorded before and after light exposure (Fig. 15b). These data show that the initial form of flavin in DpCry1 is FAD_{ox} which upon exposure to light either in an uncontrolled manner during purification under ordinary lighting or by exposure to 366 nm light following purification under yellow light is photoreduced to $FAD^{\circ-}$.

To obtain the stoichiometry of flavin in DpCry1, the protein was heat-denatured to release flavin from the apoenzyme. Since the flavin is present in at least two different forms in the native protein, heat-denaturation of DpCry1 was necessary to convert all flavin to FAD_{ox}. Additionally, heat-denaturation releases MTHF which at neutral pH undergoes cleavage of the 5,10-methenyl bond which is responsible for its absorption at 380 nm. As a consequence, denaturation at neutral pH eliminates the contribution of folate to the absorption spectra in near-UV. Therefore, the absorption of denatured protein can be solely attributed to FAD_{ox} and thus the total flavin concentration can be calculated using the extinction coefficient for FAD_{ox} at 440 nm, 11,300 $M^{-1}cm^{-1}$ (Fig. 15c). The concentration of flavin in DpCry1 ranged from 30-60 μM and the resulting flavin to protein ratio ranged from 0.7-1.0 in 30-60 μM of holoenzyme. Therefore, DpCry1 contains essentially stoichiometric amounts of flavin making it the first animal cryptochrome to be purified with greater than 5% flavin. The presence of flavin was verified in the denatured sample by fluorescence emission at 520 nm after excitation at 440 nm as well as excitation at 380 and 450 nm after emission at 520 nm; both of which are indicative of FAD_{ox} (Fig. 16a). The presence of folate in DpCry1 was measured by fluorescence emission at 460 nm after excitation of the native protein at 400 nm (Fig. 16b). Although its concentration was not calculated, it clearly exists in grossly

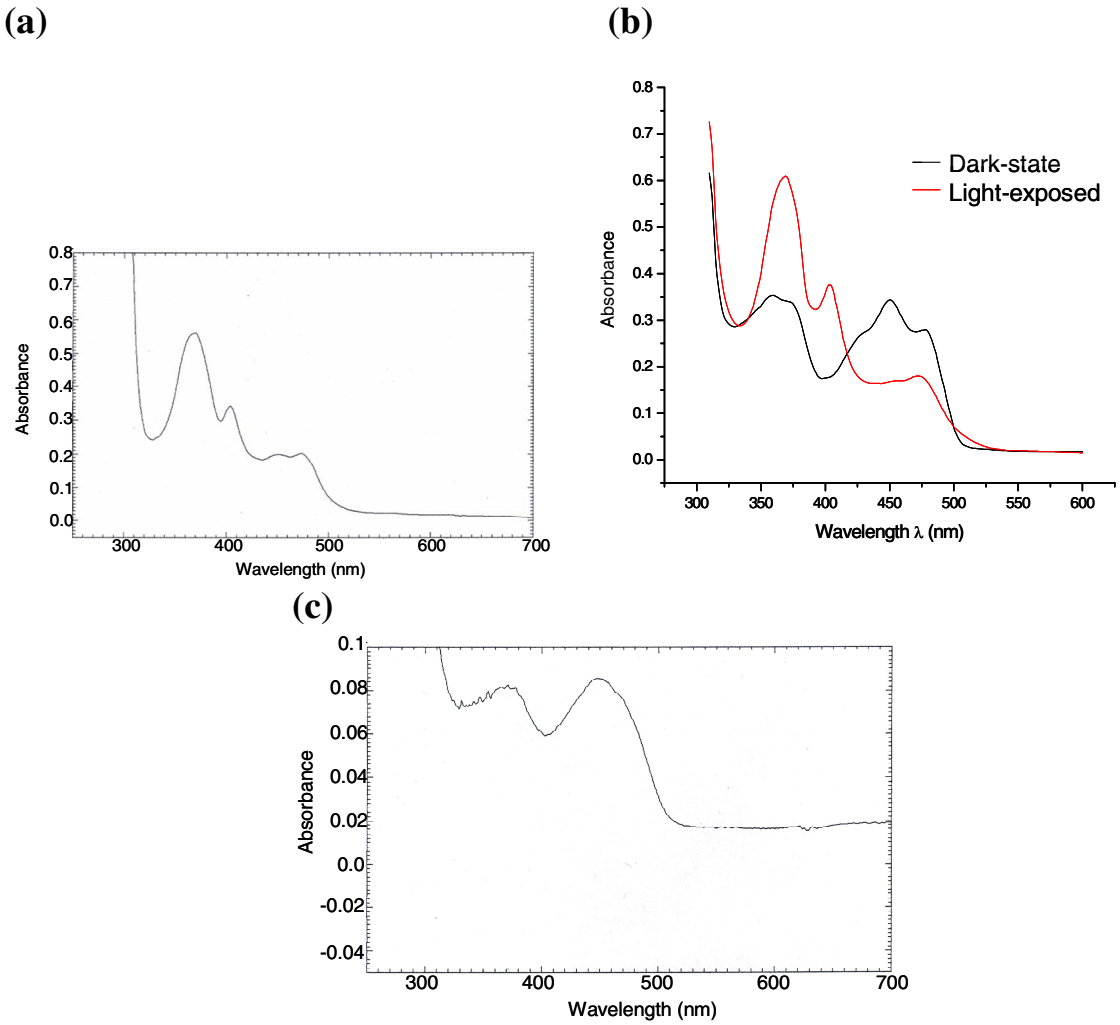

Figure 15. Absorption spectra of DpCry1. (a) Native protein absorption spectrum of recombinant MBP-DpCry1 shows the presence of the anionic semiquinone radical ($FAD^{\circ-}$) with an absorption maximum at 370 nm, a small shoulder at 405 nm, and a smaller peak at 470 nm. Presence of a small amount of fully oxidized flavin (FAD_{ox}) is observed by a peak at 450 nm in addition to its contribution to the absorption maximum at 370 nm. There is no evidence of MTHF in the native protein absorption spectrum. (b) Native protein absorption spectrum of DpCry1 purified in dark conditions was recorded to conclude that the dark-state of flavin (black) is FAD_{ox}. The absorption spectrum was recorded after the protein was exposed to light (red) to show the flavin reduction from FAD_{ox} to $FAD^{\circ-}$. (c) DpCry1 was heat-denatured and the absorption spectrum recorded. Heat denaturation converts all flavin to FAD_{ox} shown by a peak at both 370 and 450 nm. Additionally, MTHF no longer absorbs in the near-UV-visible range after heat-denaturation.

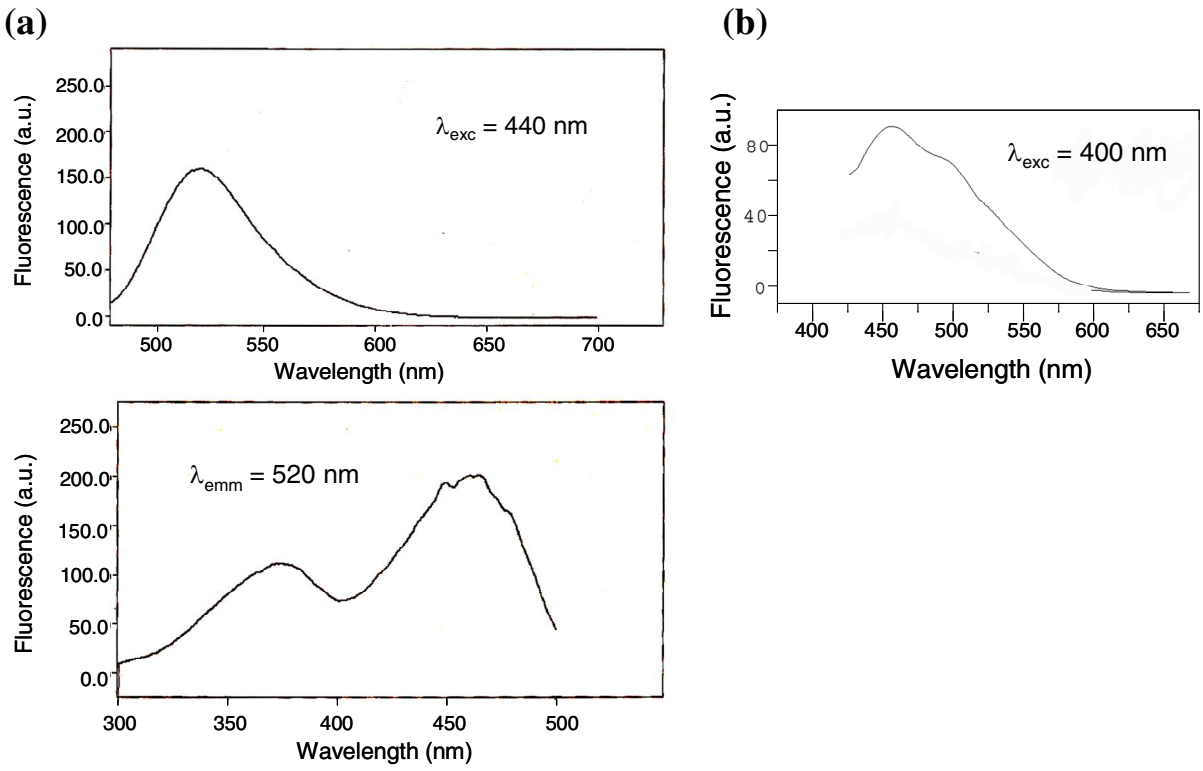

Figure. 16. Fluorescence Spectra of DpCry1. (a) Fluorescence spectra of heat- denatured DpCry1 were recorded after excitation at 440 nm (top) and emission at 520 nm (bottom) to verify the presence of flavin in DpCry1. Excitation of FAD_{ox} at 440 nm results in emission at 520 nm and emission of FAD_{ox} at 520 nm results in excitation at 370 and 450 nm. (b) Fluorescence emission of native DpCry1 at 460 nm was recorded after excitation at 400 nm showing the presence of MTHF.

sub-stoichiometric levels as indicated by its lack of contribution to the absorption spectrum of native protein (Fig. 15a).

As explained earlier, *Arabidopsis* cryptochromes which are known to function as photoreceptors, have been purified with stoichiometric flavin (65) but *Drosophila* cryptochrome, also known to function as a photoreceptor, has only been purified with less than 5% flavin (4). The lack of flavin in a recombinant protein, such as dCry, does not necessarily mean that that protein does not contain stoichiometric flavin *in vivo* because flavin incorporation is often reduced in misfolded cryptochromes expressed in heterologous systems. Additionally, since the chromophore is non-covalently bound to the protein, flavin is often lost during purification. However, the presence of flavin in a recombinant protein is very supportive of the presence of stoichiometric flavin *in vivo*. Based on the photolyase photocycle as a model for the cryptochrome photocycle, where $FADH^-$ is the catalytic chromophore, purification of a cryptochrome with stoichiometric levels of flavin is very supportive of a photoreceptive role for that protein. Therefore, these results showing that recombinant DpCry1 has stoichiometric flavin suggest that DpCry1 likely performs an important photoreceptive function in the butterfly circadian clock. While it has been shown that DpCry1 is degraded in response to light (63), there is still no published data definitively proving that it has photoreceptor activity and the data presented here provides further support that DpCry1 has a light-dependent role in the butterfly clock as a crucial blue-light photoreceptor.

Spectroscopic Characterization of DpCry2

DpCry2 was purified and characterized using methods identical to those used in DpCry1 analyses. However, spectroscopic characterization of DpCry2 showed drastically

different properties. The native protein spectrum shows only a shoulder at about 420 nm suggesting the presence of a small amount of flavin (Fig. 17a). The protein was heat-denatured to convert all existing flavin to FAD_{ox}. However, absorption was still not of sufficient magnitude to detect by our spectrophotometer (Fig. 17b). Therefore, fluorescence of the denatured protein was used to both detect and quantify the total amount of flavin (FAD_{ox}) in the protein. Similar to DpCry1, fluorescence emission of heat-denatured DpCry2 at 520 nm after excitation at 440 nm and fluorescence excitation at 380 and 440 nm after emission at 520 nm was indicative of FAD_{ox} (Fig. 18a). Comparison of the fluorescence spectra of DpCry1 (Fig. 16a) and DpCry2 (Fig. 18a) illustrates the vast difference in flavin concentration between the two proteins. Fluorescence measurements for FAD_{ox} were used against a standard curve created with known concentrations of FAD to determine the concentration of flavin in DpCry2 to be approximately 3 μM in 50 μM of protein yielding a flavin-to-protein ratio of about 0.05.

A DpCry2 truncation mutant was also purified in an attempt to isolate the recombinant protein with greater than 5% flavin, however, the characterization of this mutant led to similar results of about 0.05 flavin-to-protein ratio.

The presence of folate in DpCry2 was also assessed using fluorescence emission of the native protein after excitation at 400 nm. Similar to DpCry1, a small amount of folate was detected in the native protein by emission at 460 nm (Fig. 18b).

These results were somewhat expected based on the already established similarities between DpCry2 and other mammalian cryptochromes (63). All mammalian cryptochromes studied so far have only been definitely proven to have light-independent roles in the clock. Likewise, these proteins have never been purified with more than 5% flavin (4). However,

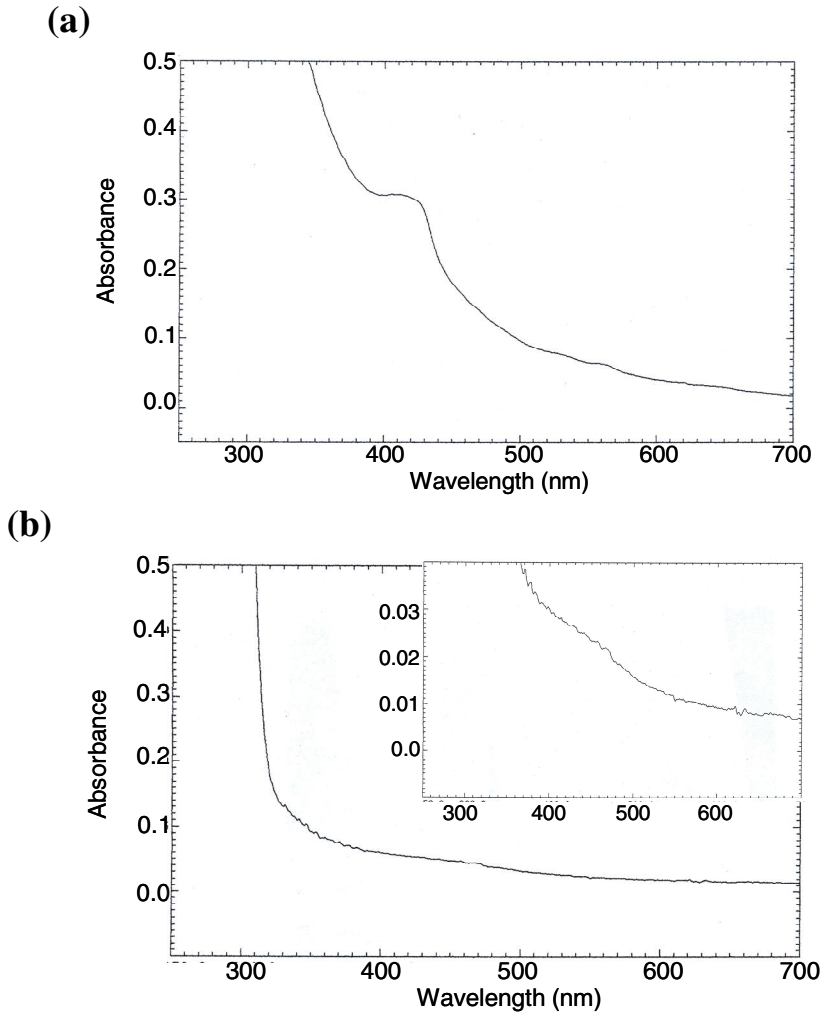

Figure 17. Absorption spectra of DpCry2. (a) Native protein absorption spectrum of recombinant MBP-DpCry2 suggests the presence of a very small amount of flavin with a shoulder at 420 nm. (b) DpCry2 was heat-denatured and the absorption spectrum recorded. The inset shows a close-up of the spectrum in the flavin-absorbing range indicating very little flavin.

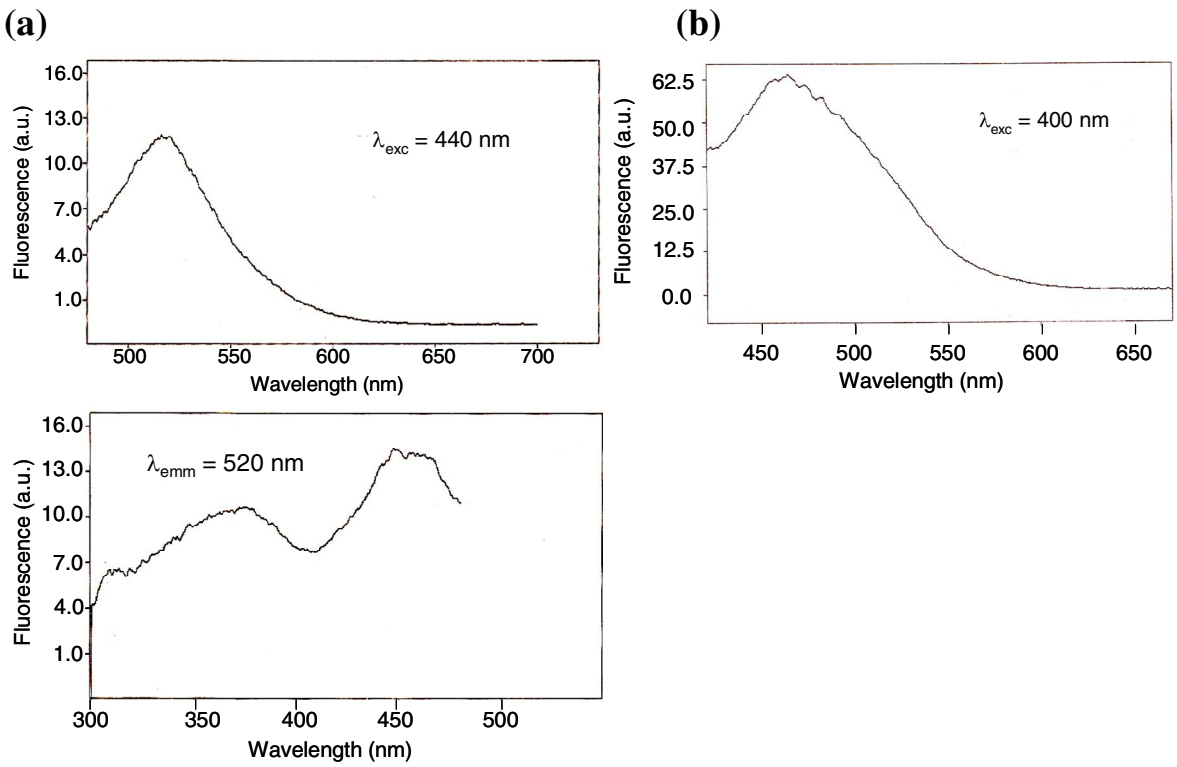

Figure 18. Fluorescence spectra of DpCry2. (a) Fluorescence spectra of heat-denatured DpCry2 were collected to verify the presence of flavin in the protein. Emission at 520 nm was shown after an excitation at 440 nm (top) while excitation at both 370 and 450 nm (bottom) was shown after an emission at 520 nm; both of which are indicative of the presence of FAD_{ox} in DpCry2. The fluorescence amplitude, however, is significantly smaller than that from DpCry1 meaning that DpCry2 contains significantly less flavin than DpCry1. (b) Fluorescence emission at 460 nm of native DpCry2 after an excitation at 400 nm is indicative of the presence of MTHF.

the lack of flavin in recombinant proteins does not necessarily mean that they do not possess the chromophore *in vivo*. Therefore, fewer conclusions can be drawn from the purification and characterization of DpCry2 based on its lack of flavin. While the photoreceptive function of mammalian cryptochromes remains elusive, there is still substantial evidence that they do have a light-dependent role in the phototransduction pathway of the circadian clock, even if that role is neither essential nor sufficient. The photoreceptive function of these cryptochromes requires further study. Unfortunately, at present, spectroscopic and biochemical analyses are of limited value due to the lack of chromophores in recombinant mammalian cryptochromes.

Spectroscopic Properties of Maltose Binding Protein

To ensure that the folate and flavin detected in MBP-DpCry1 and, in particular, in MBP-DpCry2 are intrinsic to those proteins and not due to non-specific absorption of these cofactors associated with overproduced maltose binding protein (MBP), I purified and spectroscopically characterized free MBP. Absorption spectra of both native and denatured protein showed no evidence of flavin (Fig. 19a,19b). However, when the more sensitive fluorescence spectra were recorded (Fig.19c), there was evidence of about 0.5 μM flavin (determined from a flavin standard fluorescence curve). An MBP concentration of approximately 200 μM resulted in a flavin-to-MBP ratio of less than 0.003. Therefore, we can conclude that the flavin observed in both MBP-DpCry1 and MBP-DpCry2 is intrinsic to each cryptochrome and not bound non-specifically to overexpressed MBP. Additionally, fluorescence emission at 460 nm was recorded after excitation at 400 nm to show that MBP also contains very little or no MTHF (Fig. 19d) compared to the amount seen in DpCry1 and DpCry2 (Fig. 16b,18b).

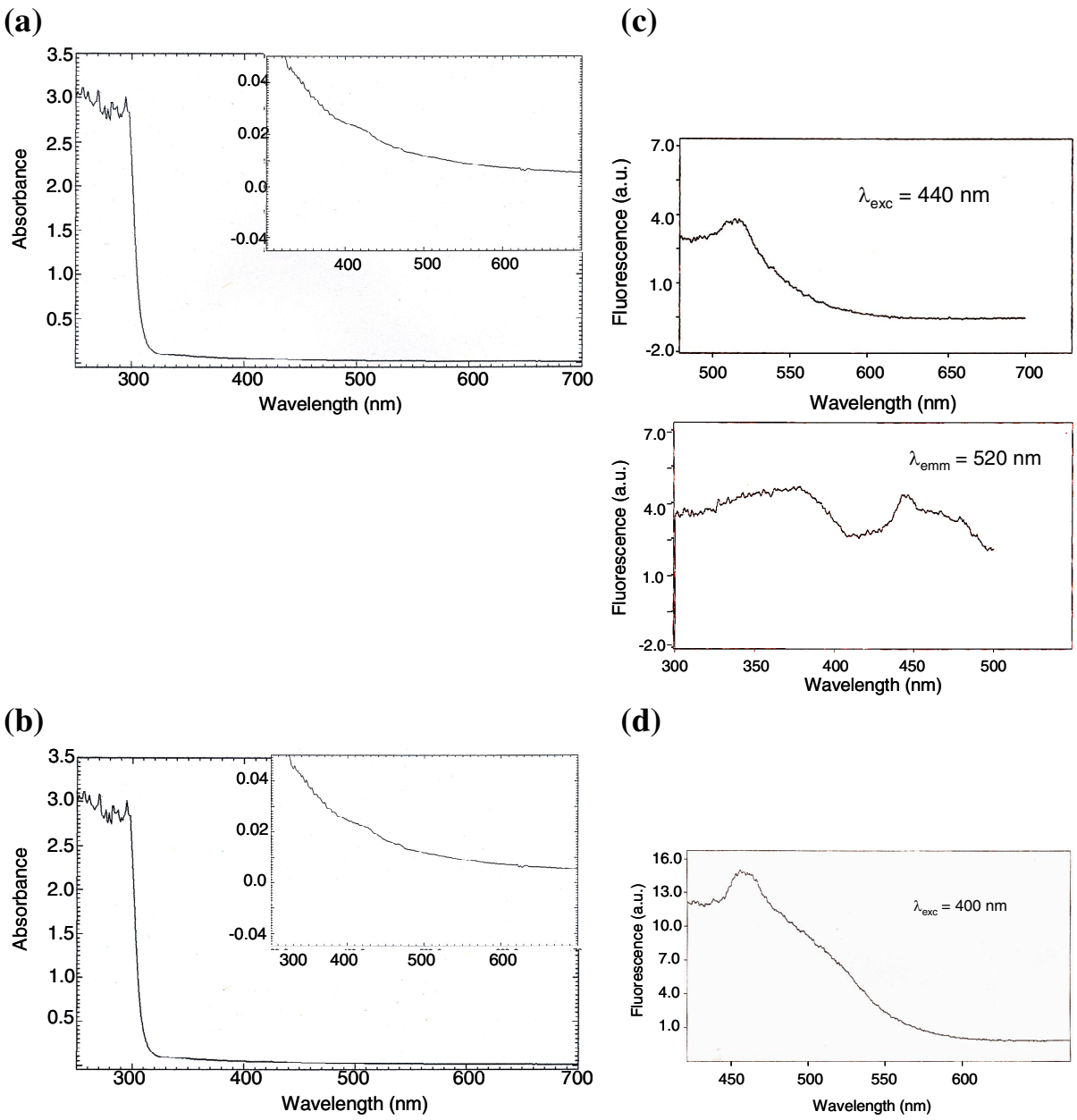

Figure 19. Absorption and fluorescence spectra of MBP. (a) Absorption spectrum of native recombinant MBP purified under identical conditions as both DpCry1 and DpCry2 showed very little chromophore (inset: close-up of flavin-absorbing region). (b) Absorption spectrum of heat-denatured MBP again showed the presence of very little FAD_{ox}. (c) Fluorescence spectra of heat-denatured MBP after excitation at 440 nm (top) and emission at 520 nm (bottom) both showed very little FAD_{ox}. The concentration of FAD_{ox} in MBP based on a flavin fluorescence standard curve was determined to be 0.5 μM, less than 0.3% in the protein. (d) Fluorescence spectrum of native MBP showed the presence of very little MTHF with a small fluorescence emission at 460 nm after excitation at 400 nm.

Autophosphorylation Activity

It has been shown that certain cryptochromes have autophosphorylating kinase activity (6). The physiological relevance of this activity that is seen most convincingly in *Arabidopsis* cryptochromes but also in human cryptochromes has been questioned as a result of recent findings (65). In an attempt to gain additional knowledge of this activity in cryptochromes, both DpCry1 and DpCry2 were tested as described previously (65). Neither DpCry1 nor DpCry2 showed any autophosphorylation when the experiment was conducted in the dark (Fig. 20). In these experiments, AtCry1 was used as a positive control (Fig. 20). Protein concentration, while not equivalent between each protein, was significantly greater for both DpCry1 and DpCry2 than for AtCry1 and thus should have favored any autophosphorylation activity of the butterfly cryptochromes if present (Fig. 20). However, the purification source and procedures for DpCry1 and DpCry2 (bacterial expression and amylose resin purification) were different than those for the AtCry1 positive control (insect cell/baculovirus expression and Ni-agarose purification) (65). Therefore, it cannot be concluded unambiguously that DpCry1 and DpCry2 do not have autophosphorylation activity. It must be noted that AtCry1 and AtCry2 have stoichiometric flavin and yet only AtCry1 has kinase activity. Of equal significance, when purified from a heterologous source hCry1 and hCry2 contain either trace amounts or no detectable flavin yet both exhibit kinase activity. Clearly, the kinase activity in cryptochromes in general and in DpCry1 and DpCry2 in particular needs further investigation.

Photophysical analysis of DpCry1

In an effort to better understand the dynamics of the flavin chromophore in DpCry1, the fluorescence lifetime of flavin in DpCry1 was analyzed by a femtosecond-resolved

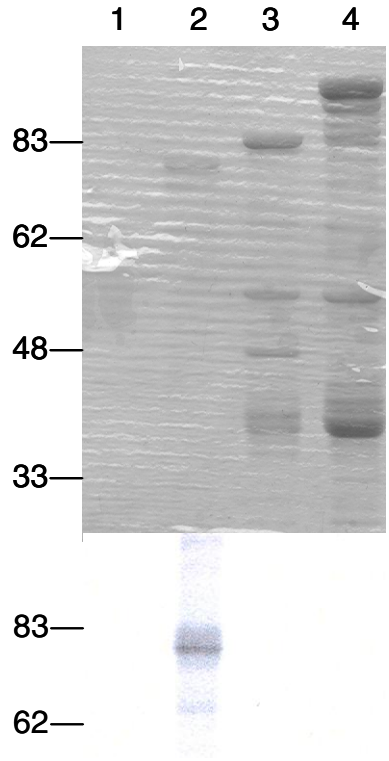

Figure 20. Autophosphorylation activity of DpCry1 and DpCry2. Lane 1: no protein negative control, lane 2: AtCry1 positive control, lane 3: MBP-DpCry1, and lane 4: MBP-DpCry2. (a) Coomassie-blue-stained gel showing protein levels used in autophosphorylation assay. (b) Phosphorimage showing the lack of autophosphorylation activity of the *Danaus plexippus* cryptochromes. Reaction conditions were identical to those described previously (65).

fluorescence up-conversion technique monitoring fluorescence at 550 nm (Fig. 21). Since flavin emits at 520 nm and MTHF emits at 460 nm, the decay of this transient should be primarily due to flavin and not MTHF. The decay curve of flavin (Fig. 21) can be best fitted to three different exponential components: 0.68 ps decay representing 79% of the amplitude, 3.9 ps decay (17%), and 175 ps (4%). The source of each decay exponential component is undefined at this point, however several speculations can be made. The shortest decay component possessing a lifetime of 0.68 ps (79%) is likely due to the decay of the anionic flavin radical since it is the most abundant redox state of flavin in recombinant DpCry1 grown under normal lighting conditions. The intermediate decay component, 3.9 ps (17%) is likely due to the small amount of oxidized flavin that is present in DpCry1 grown in these conditions. The longest decay component at 175 ps (4%) is likely from the small amount of excited flavin not bound to apoprotein that is present in the sample. While no conclusions can be made about the resonance energy transfer dynamics of DpCry1 from this data, the lifetime observed for flavin is the shortest observed among any of the proteins within the photolyase/cryptochrome family of blue-light photoreceptors and may be taken as an indication for a novel photochemical reaction pathway in cryptochromes. Additionally, with the recent discovery that VcCry1 and the entire cry-DASH subfamily is more accurately classified as a ssDNA-specific photolyase (24), the results discussed here include the first analysis of the photophysical dynamics of flavin in a bona fide cryptochrome. Future studies will likely involve analysis of the resonance energy transfer dynamics between MTHF and FAD in DpCry1 to obtain further knowledge in regards to the putative photoreceptive function of this protein.

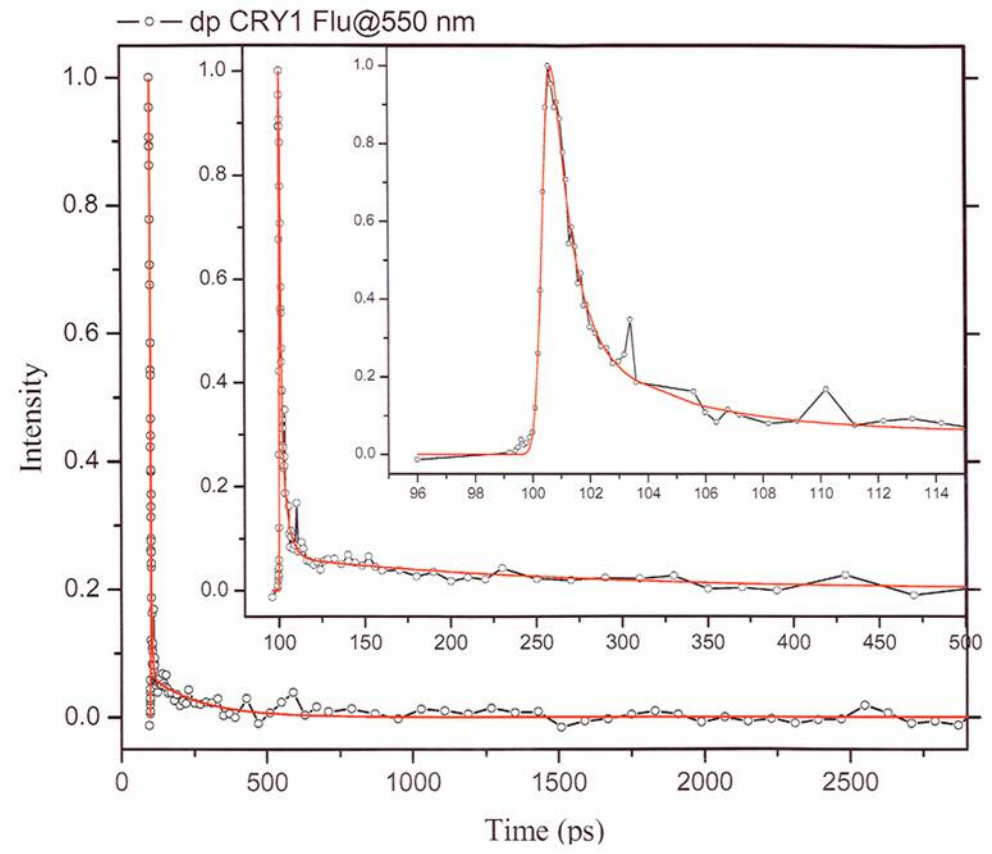

Figure 21. Fluorescence lifetime of flavin in DpCry1. Femtosecond-resolved fluorescence up-conversion technique was used to obtain a fluorescence transient at 550 nm for DpCry1. The transient shows three separate exponential decay rates of 0.68 ps, 3.9 ps, and 175 ps most likely representing the decay of $FAD^{\circ-}$, FAD_{ox}, and MTHF respectively.

Conclusion

The characterization of DpCry1 and DpCry2 has shown that DpCry1 has properties in support of a photoreceptive function and that DpCry2 shows properties similar to other mammalian cryptochromes. At present, not much can be concluded from our studies on DpCry2 since it lacks the flavin chromophore similar to other animal cryptochromes purified from heterologous expression systems. Even if these animal cryptochromes that show no light-dependent activity possess an elusive light-dependent role in the clock, biochemical methods have failed to be very effective since the recombinant proteins lack the essential catalytic chromophore necessary for photoreception. However, the purification and characterization of DpCry1 provides a unique opportunity for further biochemical studies on the first animal cryptochrome purified with stoichiometric levels of flavin. Since the butterfly cryptochromes may represent the ancestral insect clock, future study of these proteins is important towards the long-term goal to identify the photoreceptive mechanism and phototransduction pathways of cryptochromes in the circadian clock.

Acknowledgments

Some of the data presented were conducted by my coworker Dr. Sang-Hun Song (University of North Carolina, Chapel Hill) including the dark-state redox form of flavin in DpCry1 as well as the fluorescence of folate in DpCry1 after excitation at 400 nm. The photophysical studies were conducted by our collaborator, Dr. Dongping Zhong (Ohio State University) using the cryptochrome I purified in our lab.

CHAPTER 3

CONCLUSIONS AND FUTURE DIRECTIONS

Cryptochromes are essential components to the circadian clock in a wide variety of species ranging from bacteria to humans. Their potential to function as a blue-light photoreceptor within the circadian clock makes them important proteins to investigate as we try to understand more of the molecular details of the clock. Photolyase, the second member in the family of proteins to which cryptochrome belongs, has been shown to proceed through a well understood photocycle. Although the first cryptochrome was discovered over 13 years ago, the photocycle and photochemical mechanisms of cryptochrome remain ill-defined. A significant amount of work has been accomplished through genetic studies and *in vivo* experiments. However, biochemical methods have failed to yield significant information due to the difficulty of obtaining recombinant proteins that contain stoichiometric levels of the chromophores shown to be essential to the photolyase photocycle. More specifically, very little biochemical work has been accomplished for any of the animal cryptochromes since no animal cryptochrome has ever been purified with stoichiometric chromophore levels. This hurdle to the advancement of research on cryptochromes has initiated the search for other species whose cryptochromes might behave better as recombinant proteins.

The *Danaus plexippus* cryptochromes (DpCry1 and DpCry2) were recently identified and cloned. *In vivo* experiments revealed that DpCry1 behaved similar to *Drosophila* cryptochrome, a well-established photoreceptor, and DpCry2 behaved similar to other mammalian cryptochromes which function as transcription repressors of the central clock

transcriptional feedback loop. However, the biochemical properties of each protein had previously not been evaluated. The work presented in this thesis shows that DpCry1 can be purified with stoichiometric levels of the flavin chromophore, notably becoming the first recombinant animal cryptochrome to contain stoichiometric levels of any chromophore. This is an exciting finding since there is very strong evidence that DpCry1 functions as a photoreceptor. The only other animal cryptochrome shown to have photoreceptive activity is *Drosophila* cryptochrome which has never been purified with greater than 5% flavin content. The significance of this finding is increased with the recent discovery that the basal insect lineage of cryptochrome likely resembles the situation found in *D. plexippus* (one *Drosophila*-like and one mammalian-like cryptochrome) as opposed to the extensively-studied *Drosophila* cryptochrome which is now thought to have diverged from the initial basal insect lineage. Although dCry has been an excellent model, it appears DpCry1 could likely become the newest, more relevant, and more informative model for animal cryptochrome photoreceptors.

The data presented in this thesis suggest a novel photochemical mechanism for DpCry1. The light-dependent existence of the anionic radical flavin and the extremely short flavin lifetime both point towards a reaction pathway that may differ from that in photolyase. The physiological relevance of the light-dependent reduction from oxidized flavin to the anionic flavin radical will be investigated by comparison to photolyase photoreduction rates and by calculating the quantum yield of photoreduction. Additionally, for the first time, degradation of cryptochrome (DpCry1) by light will be tested *in vitro*. This has been impossible to accomplish with recombinant dCry since it lacks stoichiometric chromophores, even though it shows light-dependent degradation *in vivo*. The existence, relevance, and role

of folate will also be further investigated as will the autophosphorylation activity of both DpCry1 and DpCry2.

Without a doubt, this work has opened up the opportunity for *in vitro* biochemical and photophysical methods to be used to help identify the photocycle and photochemical mechanisms of cryptochrome. While genetic experiments provide important information about the physiological function of cryptochromes, they have not been sufficient to elucidate its photocycle. I predict that DpCry1 may soon become a newer and better animal cryptochrome model and that it is only a matter of time before we will finally identify the elusive photocycle of cryptochrome.

REFERENCES

1. Sancar, A. (2003) Structure and function of DNA photolyase and cryptochrome blue-light photoreceptors. *Chem. Rev*. **103**, 2203-2237.

2. Sancar, A. (2000) Cryptochrome: the second photoactive pigment in the eye and its role in circadian photoreception. *Annu. Rev. Biochem*. **69**, 31-67.

3. Zhao, X., Liu, J., Hsu, D. S., Zhao, S., Taylor, J. S., and Sancar, A. (1997) Reaction mechanism of (6-4) photolyase. *J. Biol. Chem*. **272**, 32580-32590.

4. Sancar, A. (2004) Regulation of the mammalian circadian clock by cryptochrome. *J. Biol. Chem*. **279**(33), 34079-34082.

5. Park, H. W., Kim, S. T., Sancar, A., and Deisenhofer, J. (1995) Crystal Structure of DNA Photolyase from *Escherichia coli*. *Science* **268**, 1866-1872.

6. Partch, C. L. and Sancar, A. (2005) Photochemistry and photobiology of cryptochrome blue-light photopigments: the search for a photocycle. *Photochem. Photobiol*. **81**,1291-1304.

7. Brudler, R., Hitomi, K., Daiyasu, H., Toh, H., Kucho, K., Ishiura, M., Kanehisa, M., Roberts, V. A., Todo, T., Tainer, J. A., and Getzoff, E. D. (2003) Identification of a new cryptochrome class. Structure, function, and evolution. *Mol. Cell* **11**, 59-67.

8. Brautigam, C. A., Smith, B. S., Ma, Z., Palnitkar, M., Tomchick, D. R., Machius, M., and Deisenhofer, J. (2004) Structure of the photolyase-like domain of cryptochrome 1 from Arabidopsis thaliana. *Proc. Natl. Acad. Sci. U S A*. **101**, 12142-12147.

9. Johnson, J. L., Hamm-Alvarez, S., Payne, G., Sancar, G. B., Rajagopalan, K. V., Sancar, A. (1988) Identification of the second chromophore of Escherichia coli and yeast DNA photolyases as 5,10-methenyltetrahydrofolate. *Proc. Natl. Acad. Sci U S A.* **85**, 2046-2050.

10. Sancar, G. B., Smith, F. W., and Heelis, P. F. (1987) Purification of the yeast PHR1 photolyase from an Escherichia coli overproducing strain and characterization of the intrinsic chromophores of the enzyme. *J. Biol. Chem*. **262**, 15457-15465.

11. Eker, A. P., Yajima, H., and Yasui, A. (1994) DNA photolyase from the fungus *Neurospora crassa.* Purification, characterization and comparison with other photolyases. *Photochem. Photobiol.* **60**, 125-133.

12. Malhotra, K., Kim, S. T., and Sancar, A. (1994) Characterization of a medium wavelength type DNA photolyase: purification and properties of photolyase from *Bacillus firmus. Biochemistry* **33**, 8712-8718.

13. Massey, V. (2000) The Chemical and Biological Versatility of Riboflavin. *Bioc. Soc. Trans*. **28**, 283-296.

14. Massey, V., and Palmer, G. (1966) On the existence of spectrally distinct classes of flavoprotein semiquinones. A new method for the quantitative production of flavoprotein semiquinones. *Biochemistry* **5**, 3181-3189.

15. Heelis, P. F. (1982) The photophysical and photochemical properties of flavins (isoalloxazines). *Chem. Soc. Rev*. **11**, 15-39.

16. Kao, Y., Saxena, C., Wang, L., Sancar, A., and Zhong, D. (2005) Direct observation of thymine dimer repair in DNA by photolyase. *Proc. Natl. Acad. Sci U S A* **102**, 16128-16132.

17. Saxena, C., Wang, H., Kavakli, H., Sancar, A., and Zhong, D. (2005) Ultrafast dynamics of resonance energy transfer in cryptochrome. *J. Am. Chem. Soc*. **127**, 7984-7985.

18. Kim, S. T., Heelis, P. F., Okamura, T., Hirata, Y., Mataga, N., and Sancar, A. (1991) Determination of rates and yields of interchromophore (folate----flavin) energy transfer and intermolecular (flavin----DNA) electron transfer in Escherichia coli photolyase by time-resolved fluorescence and absorption spectroscopy. *Biochemistry* **30**, 11262-11270.

19. Partch, C. L. (2006) Signal Transduction Mechanisms of Cryptochrome. Ph.D Thesis, University of North Carolina, Chapel Hill.

20. Cashmore, A. R., Jarillo, J. A., Wu, Y. J., and Liu, D. (1999) Cryptochromes: blue light receptors for plants and animals. *Science* **284**, 760-765.

21. Daiyasu, H., Ishikawa, T., Kuma, K., Iwai, S., Todo, T., and Toh, H. (2004) Identification of cryptochrome DASH from vertebrates. *Genes Cells* **9**, 479-495.

22. Hitomi, K., Okamoto, K., Daiyasu, H., Miyashita, H., Iwai, S., Toh, H., Ishiura, M., and Todo, T. (2000) Bacterial cryptochrome and photolyase: characterization of two photolyase-like genes of *Synechocystis sp*. PCC6803. *Nuc. Acids Res.* **28**, 2352-2362.

23. Worthington, E. N., Kavakli, I. H., Berrocal-Tito, G., Bondo, B. E., and Sancar, A. (2003) Purification and characterization of three members of the photolyase/cryptochrome family of blue-light photoreceptors from *Vibrio cholerae*. *J. Biol. Chem*. **278**, 39143-39154.

24. Selby, C. P. and Sancar, A. (2006) A cryptochrome/photolyase class of enzymes with single-stranded DNA-specific photolyase activity. *Proc. Natl. Acad. Sci. U S A.* **103**, 17696-17700.

25. Huang, Y., Baxter, R., Smith, B. S., Partch, C. L., Colbert, C. L., and Deisenhofer, J. (2006) Crystal structure of cryptochrome 3 from Arabidopsis thaliana and its implications for photolyase activity. *Proc. Nat. Acad. Sci*. **103**, 17701-17706.

26. Hsu, D. S., Zhao, X., Zhao, S., Kazantsev, A., Wang, R. P., Todo, T., Wei, Y. F., and Sancar, A. (1996) Putative human blue-light photoreceptors hCRY1 and hCRY2 are flavoproteins. *Biochemistry*. **35**, 13871-13877.

27. Thresher, R. J., Vitaterna, M. H., Miyamoto, Y., Kazantsev, A., Hsu, D. S., Petit, C., Selby, C. P., Dawut, L., Smithies, O., Takahashi, J. S., and Sancar, A. (1998) Role of mouse cryptochrome blue-light photoreceptor in circadian photoresponses. *Science*. **282**, 1490-1494.

28. Rubin, E. B., Shemesh, Y., Cohen, M., Elgavish, S., Robertson, H. M., and Block, G. (2006) Molecular and phylogenetic analyses reveal mammalian-like clockwork in the honey bee (*Apis mellifera*) and shed new light on the molecular evolution of the circadian clock. *Genome Res.* **16**, 1352-1365.

29. Ahmad, M. and Cashmore, A. R. (1993) HY4 gene of *A. thaliana* encodes a protein with characteristics of a blue-light photoreceptor. *Nature*. **366**,162-166.

30. Malhotra, K., Kim, S. T., Batschauer, A., Dawut, L., and Sancar, A. (1995) Putative blue-light photoreceptors from *Arabidopsis thaliana* and *Sinapis alba* with a high degree of sequence homology to DNA photolyase contain the two photolyase cofactors but lack DNA repair activity. *Biochemistry*. **34**, 6892-6899.

31. Lin, C., Robertson, D. E., Ahmad, M., Raibekas, A. A., Jorns, M. S., Dutton, P. L., and Cashmore, A. R. (1995) Association of flavin adenine dinucleotide with the *Arabidopsis* blue light receptor CRY1. *Science*. **269**, 968-970.

32. Hoffman, P. D., Batschauer, A., and Hays, J. B. (1996) PHH1, a novel gene from *Arabidopsis thaliana* that encodes a protein similar to plant blue-light photoreceptors and microbial photolyases. *Mol. Gen. Gene*. **253**, 259-265.

33. Lin, C., Yang, H., Guo, H., Mockler, T., Chen, J., and Cashmore, A. R. (1998) Enhancement of blue-light sensitivity of *Arabidopsis* seedlings by a blue light receptor cryptochrome 2. *Proc. Natl. Acad. Sci. U S A*. **95**, 2686-2690.

34. Guo, H., Yang, H., Mockler, T. C., and Lin, C. (1998) Regulation of flowering time by *Arabidopsis* photoreceptors. *Science* **279**, 1360-1363.

35. El-Din El-Assal, S., Alonso-Blanco, C., Peeters, A. J., Raz, V., and Koornneef, M. (2001) A QTL for flowering time in *Arabidopsi*s reveals a novel allele of CRY2. *Nat. Genet.* **29**, 435-440.

36. Ma, L., Li, J., Qu, L., Hager, J., Chen, Z., Zhao, H., and Deng, X. W. (2001) Light control of *Arabidopsis* development entails coordinated regulation of genome expression and cellular pathways. *Plant Cell*. **13**, 2589-2607.

37. Folta, K. M., Pontin, M. A., Karlin-Neumann, G., Bottini, R., and Spalding, E. P. (2003) Genomic and physiological studies of early cryptochrome 1 action demonstrate roles for

auxin and gibberellin in the control of hypcotyl growth by blue light. *Plant J*. **36**, 203-214.

38. Yang, H. Q., Tang, R. H., and Cashmore, A. R. (2001) The signaling mechanism of *Arabidopsis* CRY1 involves direct interaction with COP1. *Plant Cell* **13**, 2573-2587.

39. Duek, P. D., Elmer, M. W., van Oosten, V. R., and Fankhauser, C. (2004) The degradation of HFR1, a putative bHlH class transcription factor involved in light signaling, is regulated by phosphorylation and requires COP1. *Curr. Biol.* **14**, 22296-22301.

40. von Arnim, A. G., Osterlund, M. T., Kwok, S. F., and Deng, X. W. (1997) Genetic and developmental control of nuclear accumulation of COP1, a repressor of photomorphogenesis in *Arabidopsis*. *Plant Physiol.* **114**, 779-788.

41. Osterlund, M. T. and Deng, X. W. (1998) Multiple photoreceptors mediate the light-induced reduction of GUS-COP1 from *Arabidopsis* hypocotyl nuclei. *Plant J.* **16**, 201-208.

42. Subramanian, C., Kim, B. H., Lyssenko, N. N., Xu, X., Johnson, C. H., and von Arnim, A. G. (2004) The *Arabidopsis* repressor of light signaling, COP1, is regulated by nuclear exclusion: mutational analysis by bioluminescence resonance energy transfer. *Proc. Natl. Acad. Sci. U S A* **101**, 6798-6802.

43. Wang, H., Ma, L. G., Li, J. M., Zhao, H. Y., and Deng, X. W. (2001) Direct interaction of *Arabidopsis* cryptochromes with COP1 in light control development. *Science* **294**, 154-158.

44. Ang, L. H., Chattopadhyay, S., Wei, N., Oyama, T., Okada, K., Batschauer, A., and Deng, X. W. (1998) Molecular interaction between COP1 and HY5 defines a regulatory switch for light control of *Arabidopsis* development. *Mol. Cell.* **1**, 213-222.

45. Zimmerman, W. F., and Goldsmith, T. H. (1971) Photosensitivity of the circadian rhythm and of visual receptors in carotenoid-depleted *Drosophila*. *Science*. **171**, 1167-1169.

46. Frank, K. D., and Zimmerman, W. F. (1969) Action spectra for phase shifts of circadian rhythm in *Drosophila*. *Science*. **163**, 688-689.

47. Klemm, E. and Ninneman, H. (1976) Detailed action spectrum for the delay shift in pupae emergence of *Drosophila pseudoobscura*. *Photochem. Photobiol*. **24**, 369-371.

48. Ebihara, S. and Tsuji, K. (1980) Entrainment of the circadian activity rhythm to the light cycle: effective light intensity for a Zeitgeber in the retinal degenerate C3H mouse and the normal C57BL mouse. *Physiol. Behav*. **24**, 523-527.

49. Stanewsky, R., Kaneko, M., Emery, P., Beretta, B., Wager-Smith, K., Kay, S. A., Rosbash, M., and Hall, J. C. (1998) The cryb mutation identifies cryptochrome as a circadian photoreceptor in *Drosophila*. *Cell.* **95**, 681-692.

50. Emery, P., Stanewsky, R., Hall, J. C., and Rosbash, M. (2000) A unique circadian-rhythm photoreceptor. *Nature*. **404**, 456-457.

51. Rosato, E., Codd, V., Mazzotta, T., Piccin, A., Zordan, M., Costa, R., and Kyriacou, C. P. (2001) Light-dependent interaction between *Drosophila* CRY and the clock protein PER mediated by the carboxy terminus of CRY. *Curr. Biol*. **11**, 909-917.

52. Dissel, S., Codd, V., Fedic, R., Garner, K. J., Costa, R., Kyriacou, C. P., and Rosato, E. (2004) A constitutively active cryptochrome in *Drosophila melanogaster*. *Nat. Neurosci*. **7**, 834-840.

53. Busza, A., Emery-Le, M., Rosbash, M., and Emery, P. (2004) Roles of the two *Drosophila* CRYPTOCHROME structural domains in circadian photoreception. *Science*. **304**, 1503-1506.

54. Lin, F. J., Song, W., Meyer-Bernstein, E., Naidoo, N., and Sehgal, A. (2001) Photic signaling by cryptochrome in *Drosophila* circadian system. *Mol. Cell Biol*. **21**, 7287-7294.

55. Griffin, E. A. Jr., Staknis, D., and Weitz, C. J. (1999) Light-independent role of CRY1 and CRY2 in mammalian circadian clock. *Science*. **286**, 768-771.

56. Vitaterna, M. H., Selby, C. P., Todo, T., Niwa, H., Thompson, C., Fruechte, E. M., Hitomi, K., Thresher, R. J., Ishikawa, T., Miyazaki, J., Takayashi, J. S., and Sancar, A. (1999) Differential regulation of mammalian period genes and circadian rhythmicity by cryptochromes 1 and 2. *Proc. Natl. Acad. Sci. U. S. A*. **96**, 12114-12118.

57. Selby, C. P., Thompson, C., Schmitz, T. M., Van Gelder, R. N., and Sancar, A. (2000) Functional redundancy of cryptochromes and classical photoreceptors for nonvisual ocular photoreception in mice. *Proc. Natl. Acad. Sci. U S A*. **97**, 14697-14702.

58. Thompson, C. L., Selby, C. P., Partch, C. L., Plante, D. T., Thresher, R. J., Araujo, F., and Sancar, A. (2004) Further evidence for the role of cryptochromes in retinohypothalamic photoreception/phototransduction. *Brain Res. Mol. Brain Res*. **122**, 158-166.

59. Panda, S., Provencio, I., Tu, D. C., Pires, S. S., Rollag, M. D., Castrucci, A. M., Pletcher, M. T., Sato, T. K., Wiltshire, T., Andahazy, M., Kay, S. A., Van Gelder, R. N., and Hogenesch, J. B. (2003) Melanopsin is required for non-image-forming photic responses in blind mice. *Science*. **301**, 525-527.

60. Hattar, S., Lucas, R. J., Mrosovsky, N., Thompson, S., Douglas, R. H., Hankins, M. W., Lem, J., Biel, M., Hofmann, F., Forster, R. G., and Yau, K, W. (2003) Melanopsin and rod-cone photoreceptive systems account for all major accessory visual functions in mice. *Nature*. **424**, 76-81.

61. Collins, B., Mazzoni, E. O., Stanewsky, R., and Blau, J. (2006) Drosophila CRYPTOCHROME is a circadian transcriptional repressor. *Curr. Biol*. **16**, 441-449.

62. Sauman, I., Biscoe, A. D., Zhu, H., Shi, D., Froy, O., Stalleicken, J., Yuan, Q., Casselman, A., and Reppert, S. M. (2005) Connecting the navigational clock to sun compass input in monarch butterfly brain. *Neuron*. **46**, 457-467.

63. Zhu, H., Yuan, Q., Froy, O., Casselman, A., and Reppert, S. M. (2005) The two CRYs of the butterfly. *Curr. Biol*. **15**(23), 953-954.

64. Sancar, G. B. and Sancar, A. (2006) Purification and characterization of DNA photolyases. *Methods Enzymol.* **408**, 121-156.

65. Özgür, S. and Sancar, A. (2006) Analysis of autophosphorylating kinase activities of *Arabidopsis* and human cryptochromes. *Biochemistry* **45**, 13369-13374.

66. Selby, C. P. and Sancar, A. (1999) A third member of the photolyase/blue-light photoreceptor family in *Drosophila*: a putative circadian photoreceptor. *Photochem. Photobiol*. **69**, 105-107.

67. Okano, S., Kanno, S., Takao, M., Eker, A. P. M., Isono, K., Tsukahara, Y., and Yasui, A. (1999) A putative blue-light receptor from *Drosophila melanogaster*. *Photochem. Photobiol*. **69**, 108-113.

68. Shalitin, D., Yang, H., Mockler, T. C., Maymon, M., Guo, H., Whitelam, G. C., and Lin, C. (2002) Regulation of Arabidosis cryptochrome 2 by blue-light-dependent phosphorylation. *Nature* **417**, 763-767.

69. Shalitin, D., Yu, X., Maymon, M., Mockler, T., and Lin, C. (2003) Blue light-dependent *in vivo* and *in vitro* phosphorylation of *Arabidopsis* cryptochrome 1. *Plant Cell.* **15**, 2421-2429.

70. Bouly, J. P., Giovani, B., Djamei, A., Mueller, M., Zeugner, A., Dudkin, E. A., Batschauer, A. and Ahmad, M. (2003) Novel ATP-binding and autophosphorylation activity associated with *Arabidopsis* and human cryptochrome-1. *Eur. J. Biochem*. **270**, 2921-2928.

71. Saxena, C., Sancar, A., and Zhong, D. (2004) Femtosecond dynamics of DNA photolyase: energy transfer of antenna initiation and electron transfer of cofactor reduction. *J. Phys. Chem.* **108**, 18026-18033.